united nations educational, scientific and cultural organization

international atomic energy agency

the
abdus salam
international centre for theoretical physics

SMR 1232 - 18

XII WORKSHOP ON
STRONGLY CORRELATED ELECTRON SYSTEMS

17 - 28 July 2000

MAGNETO-TRANSPORT PROPERTIES AND CHARGED STRIPES IN HIGH Tc CUPRATES

Yoichi ANDO
Central Research Institute of Electric Power Industry
201-8511 Tokyo, Japan

These are preliminary lecture notes, intended only for distribution to participants.

XII Workshop on Strongly Correlated Electron Systems, ICTP, Trieste. 17-28 July 2000

Magneto-Transport Properties and Charged Stripes in High-T_c Cuprates

Yoichi Ando

Central Research Institute of Electric Power Industry (CRIEPI)

Outlines

- Phase Diagram

  .... Metal-Insulator Crossover in the Normal State
- "Anomalous Insulator"
- "Anomalous Metal"
- Possible Role of Stripes

Collaborators

A. N. Lavrov
J. Takeya
S. Komiya
K. Segawa
S. Ono

... CRIEPI

T. Murayama
Y. Abe
K. Nakamura
Y. Hanaki
N. Miyamoto

... Science Univ. Tokyo / CRIEPI

G. S. Boebinger
F. F. Balakirev
J. B. Betts

...NHMFL, Los Alamos National Lab.

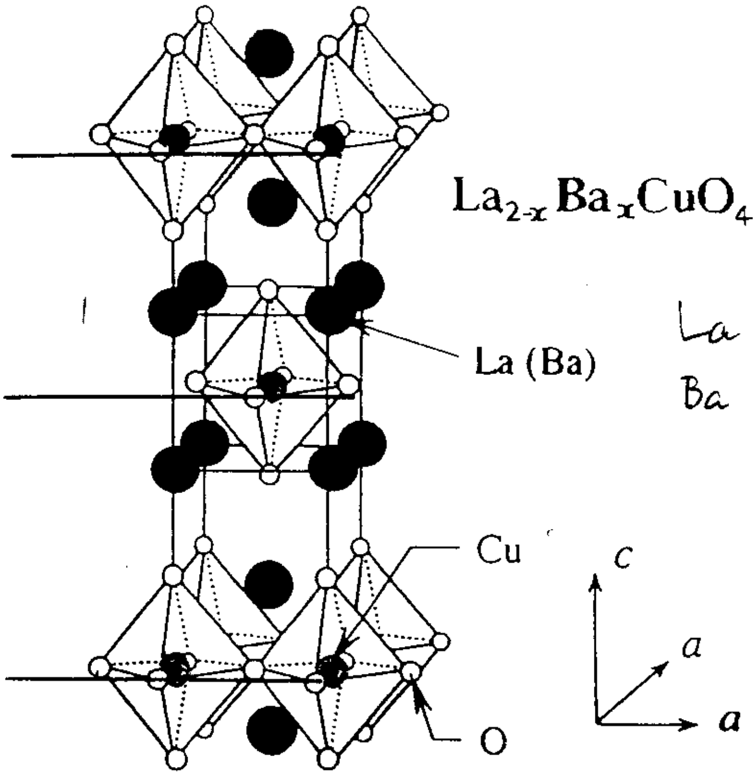

La ion is 3+
Ba ion is 2+

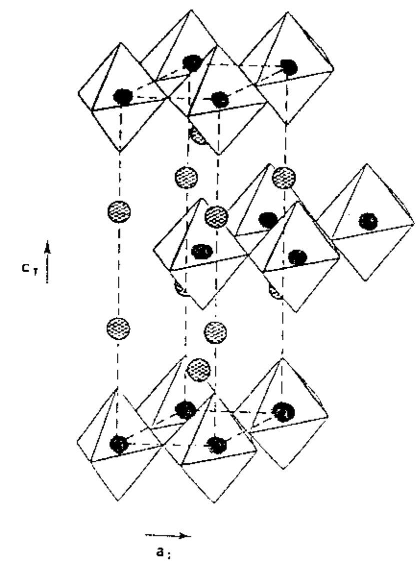

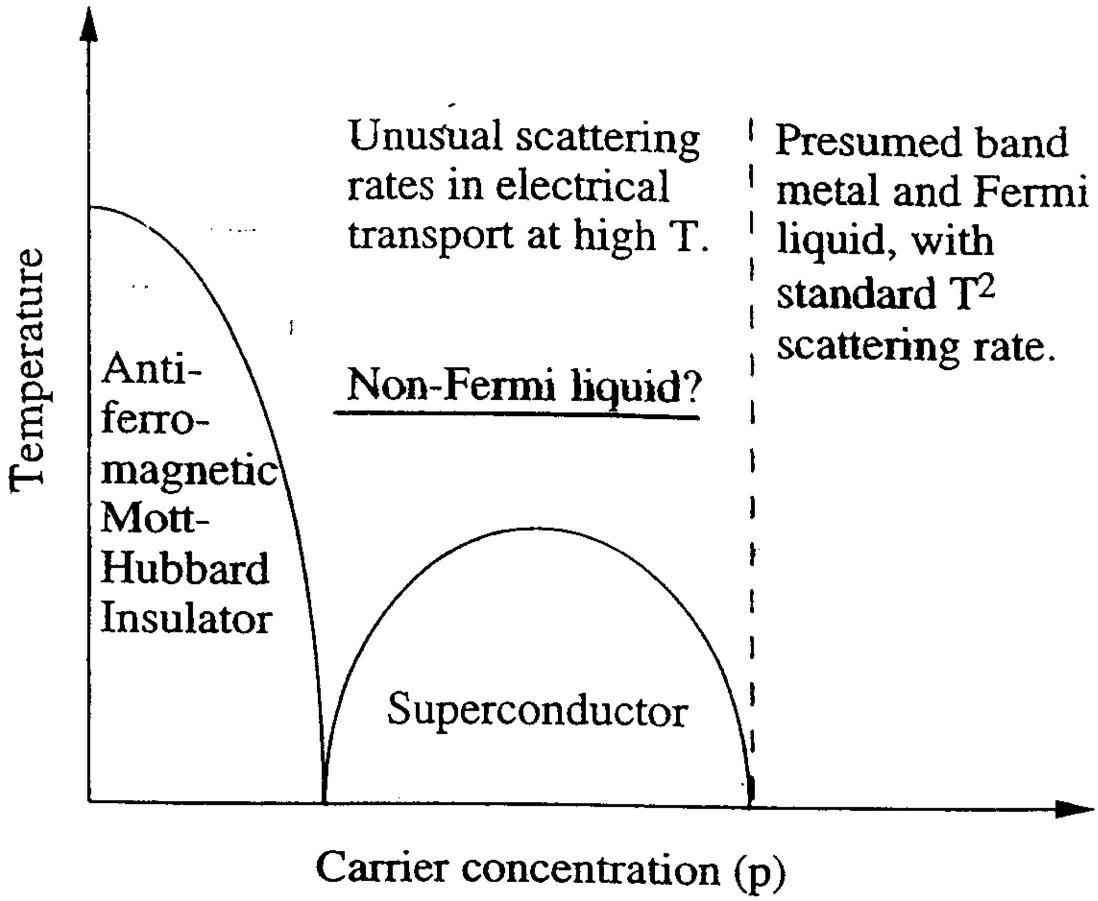
Temperature
Anti-
ferro-
magnetic
Mott-
Hubbard
Insulator
Unusual scattering rates in electrical transport at high T.
Non-Fermi liquid?
Superconductor
Presumed band metal and Fermi liquid, with standard T2 scattering rate.
Carrier concentration (p)

$La_{2-x}Sr_xCuO_4$

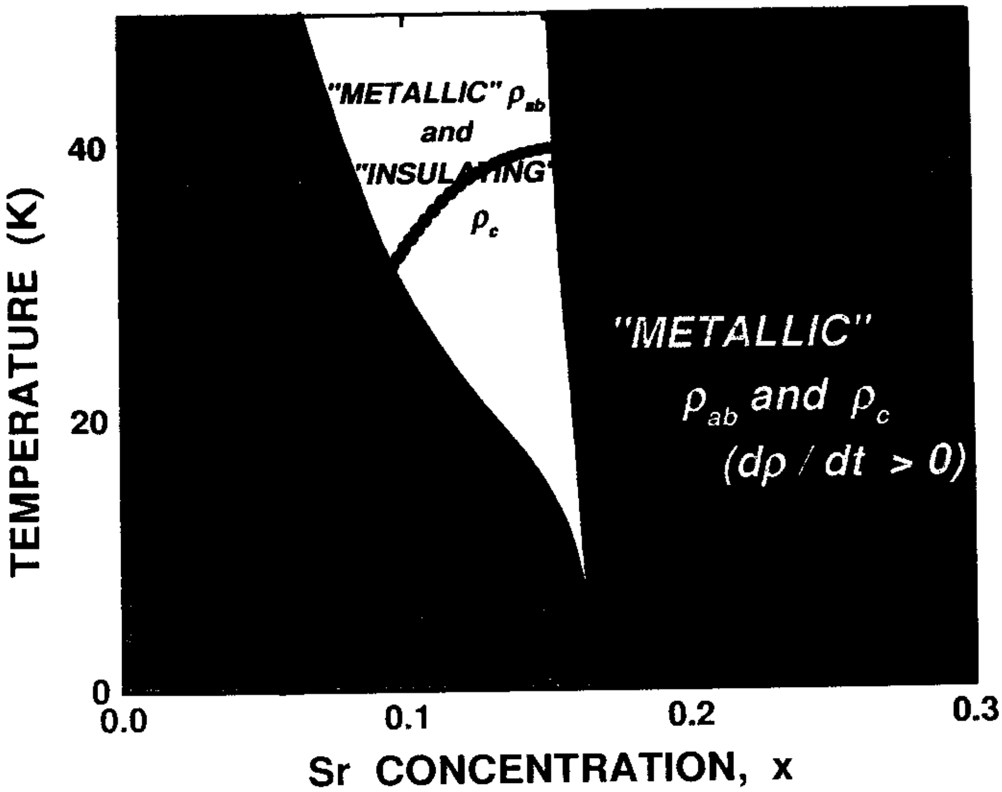

PRL 77, 5417 (1996).

Charge confinement is broken?

or

Confined charge is localizing?

For 2D free electrons, $k_F l \simeq h c_0 / \rho e^2$ ($c_0 = 6.5$ Å)

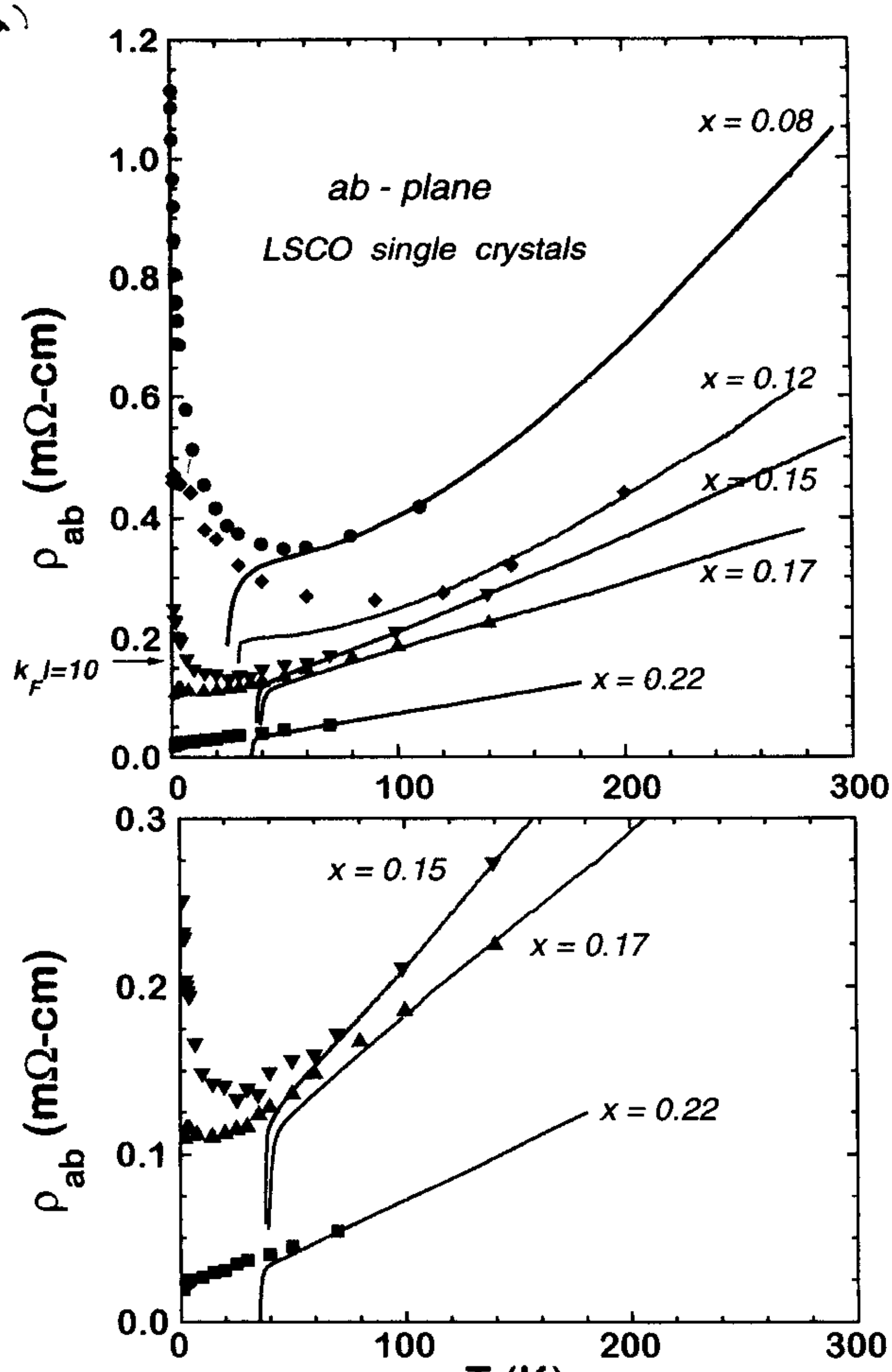

$Pr_{2-x}Ce_xCuO_4$

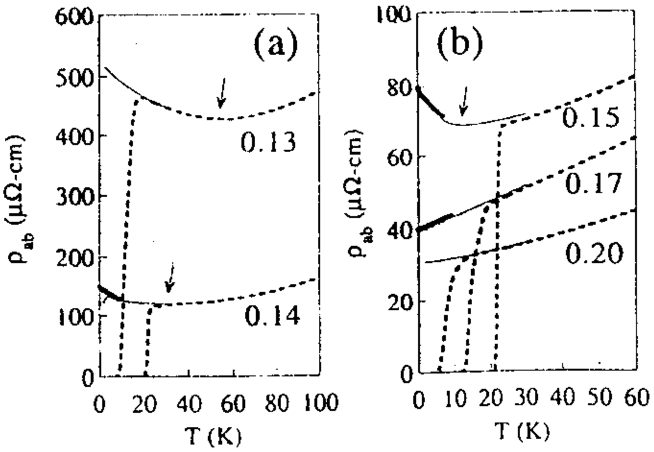

FIG. 1. Resistivity ρ_{ab} as a function of temperature for the c-axis oriented $Pr_{2-x}Ce_xCuO_4$ thin films in magnetic fields of 0 T (dashed lines), 8.7 T (thin lines), and 12 T (thick lines). (a) $x = 0.13$ and 0.14; (b) $x \geq 0.15$. The field is applied along the c axis.

P. Fournier et al.

PRL 81, 4720 (1998).

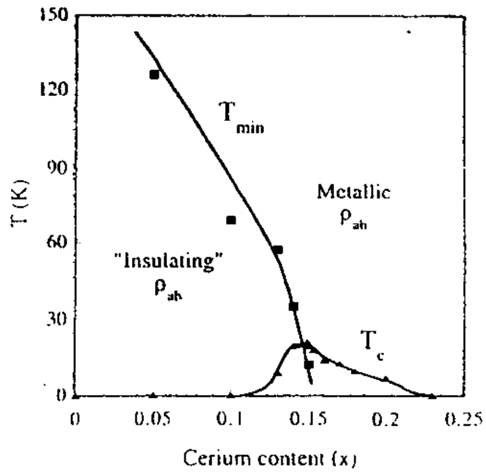

FIG. 3. Phase diagram determined from resistivity data of $Pr_{2-x}Ce_xCuO_4$ thin films. Solid triangles and solid squares are T_c and T_{min} (defined in text), respectively. The solid lines are guides to the eye.

LSCO $x = 0.10$ (underdoped)

Strained Films

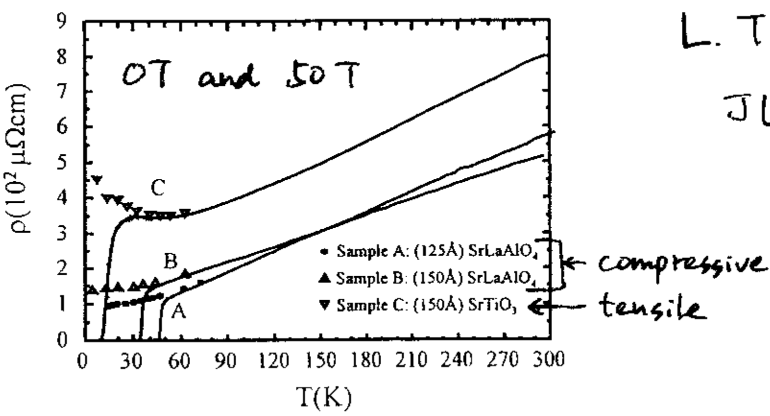

L. Trappeniers

JLTP 117, 681 (1999).

$Bi_2Sr_{2-x}La_xCuO_{6+\delta}$ (La-doped Bi-2201)

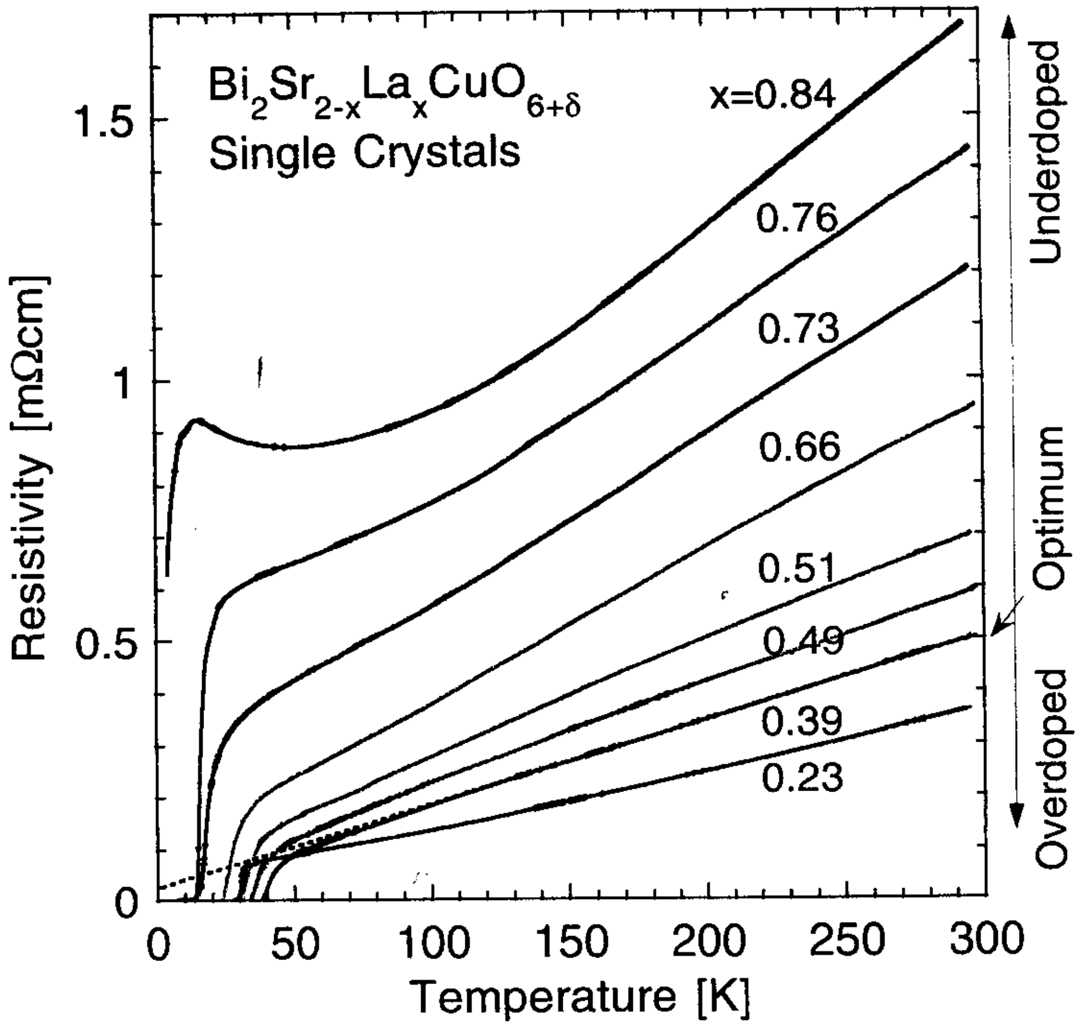

Optimally-doped sample:

Optimum T_c = 38 K

Residual resistivity ~20 μΩcm

PRB 61, R14956 (2000).

$R_H eN/V$ ... Inverse of the "fictitious" hole density per Cu

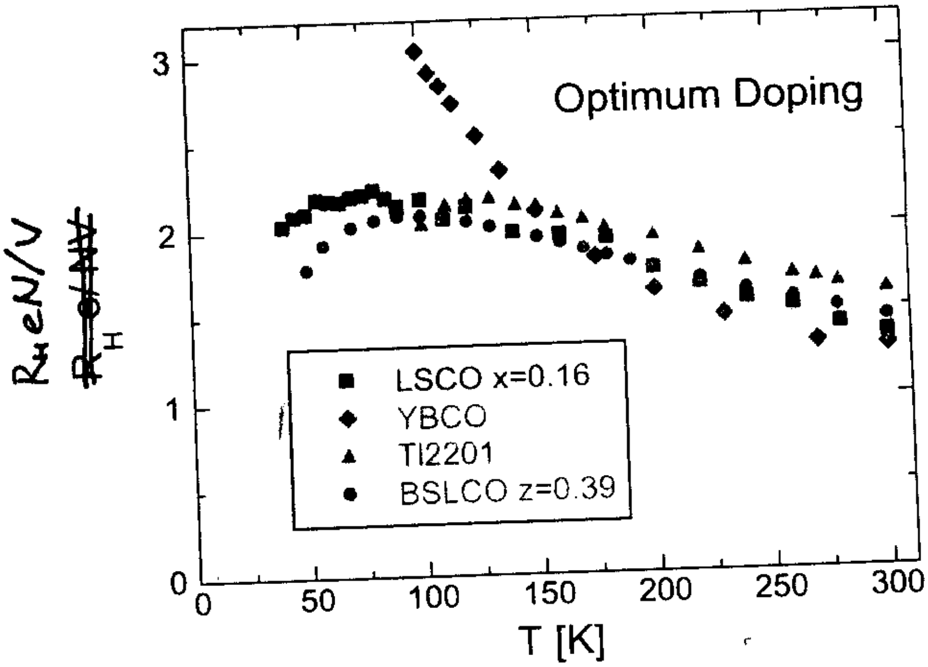

$R_H = \frac{1}{ne}$

$n = \frac{1}{R_H e}$

$n \times \left(\frac{V}{N}\right) = \frac{V}{R_H e N}$

$\therefore R_H eN/V = \left\{ n \times \left(\frac{V}{N}\right) \right\}^{-1}$

↑ hole density per Cu.

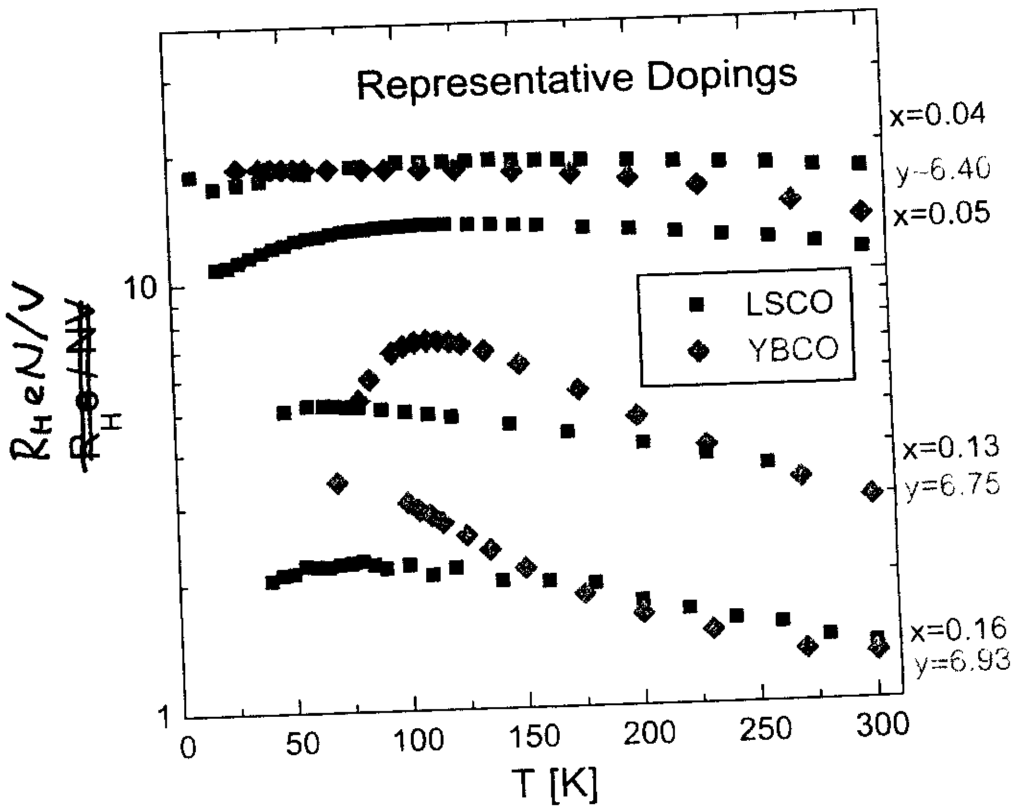

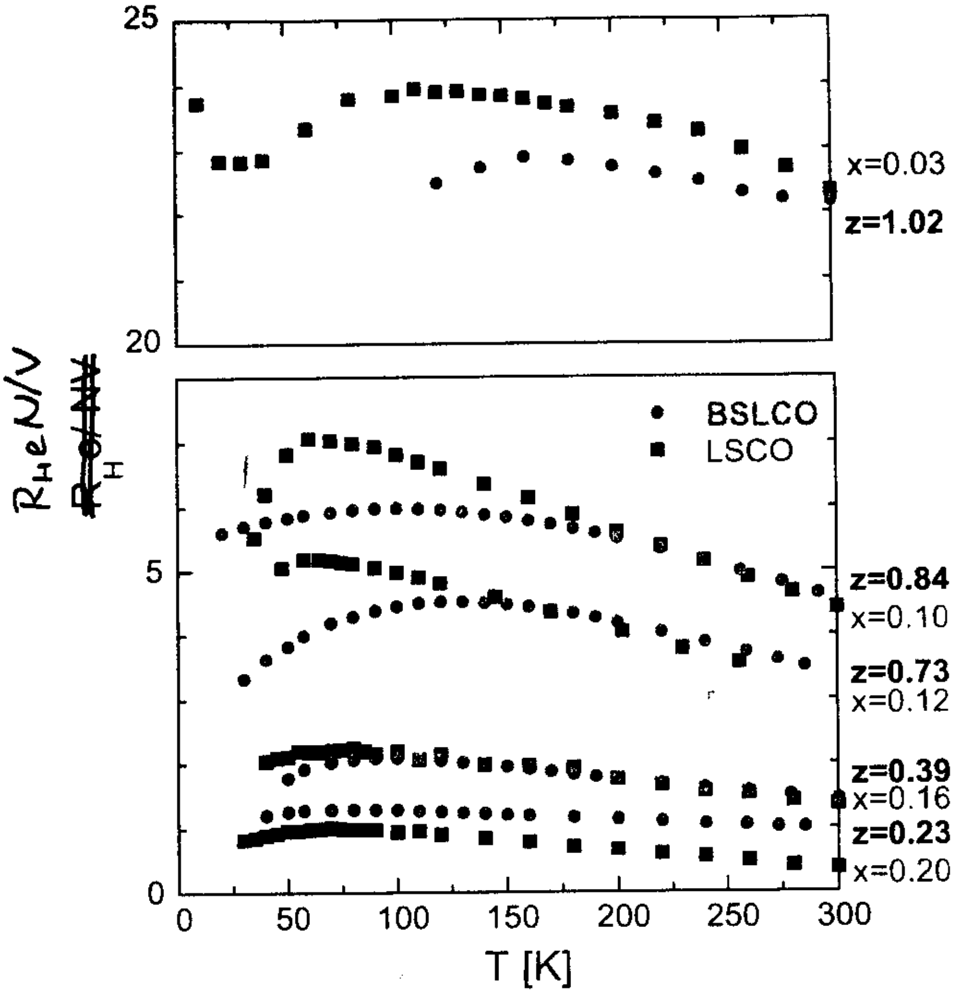

25
20
5
0
0
50
100
150
200
250
300
T [K]
BSLCO
LSCO
x=0.03
z=1.02
z=0.84
x=0.10
z=0.73
x=0.12
z=0.39
x=0.16
z=0.23
x=0.20

$Bi_2Sr_{2-z}La_zCuO_{6+\delta}$

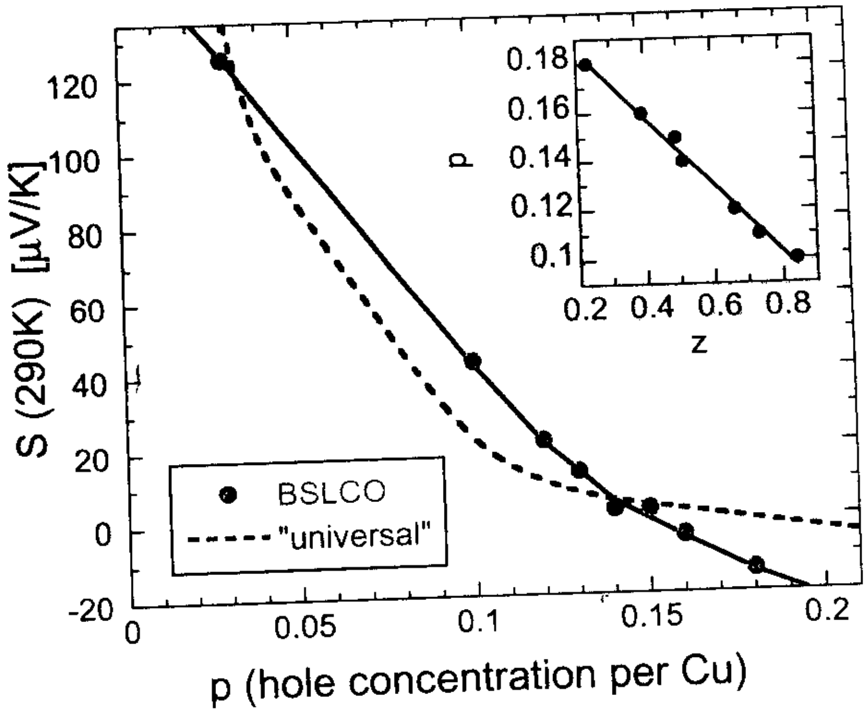

$Bi_2Sr_{2-x}La_xCuO_{6+\delta}$ in 0 and 60 T

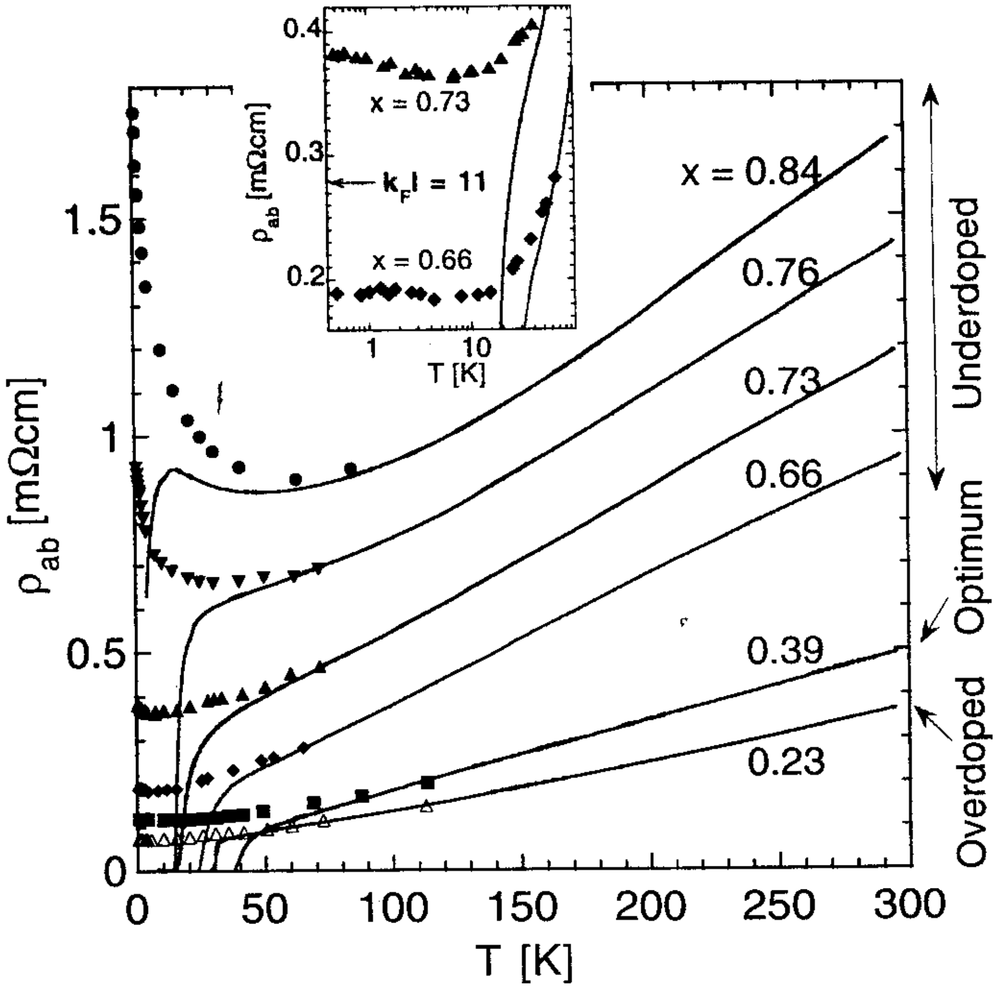

MI crossover takes place in the **underdoped region**, not at **optimum doping**.

Phase diagram of BSLCO

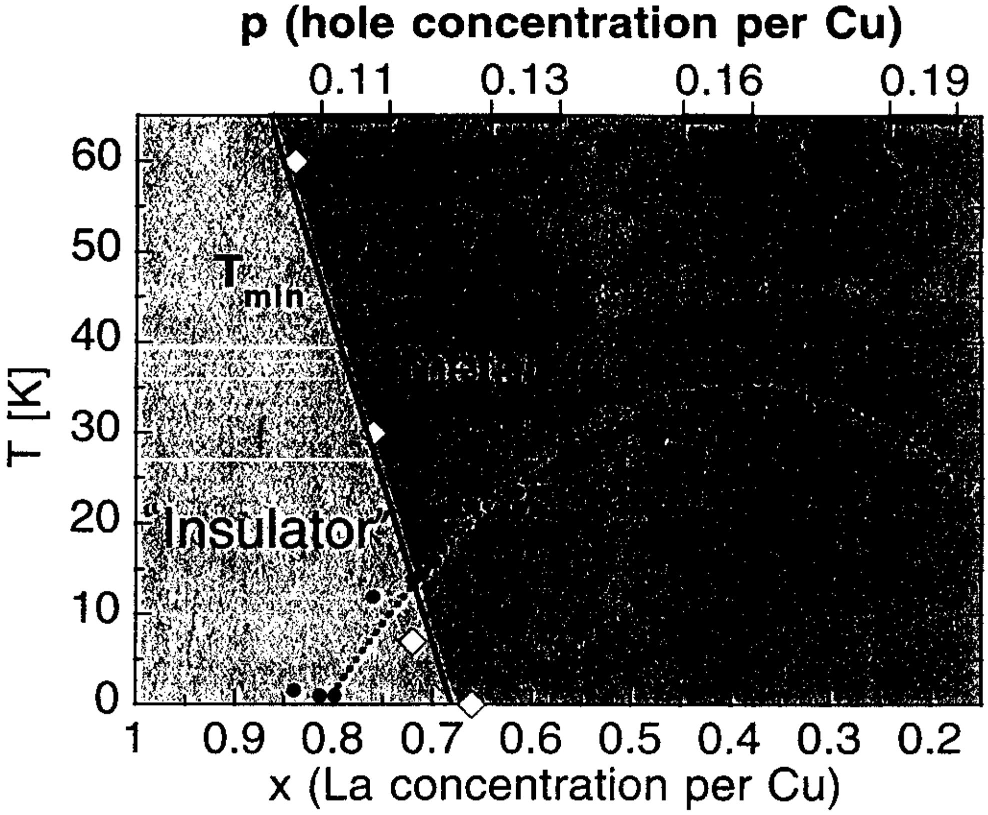

MI crossover of BSLCO is estimated to take place around **p ~ 1/8**

S. Ono, Y. Ando, ...

PRL 85, 638 (2000)

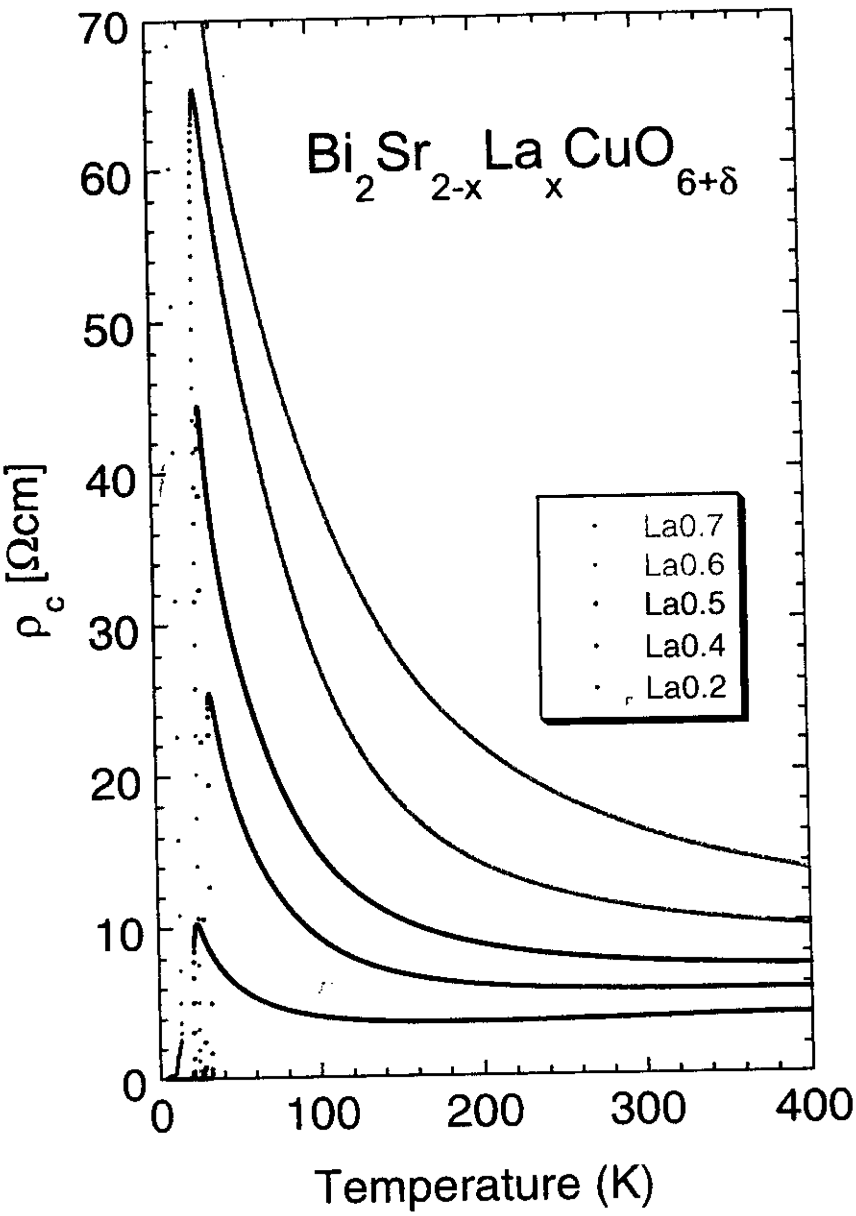

$Bi_2Sr_{2-x}La_xCuO_{6+\delta}$
La0.7
La0.6
La0.5
La0.4
La0.2
ρ_c [Ωcm]
Temperature (K)

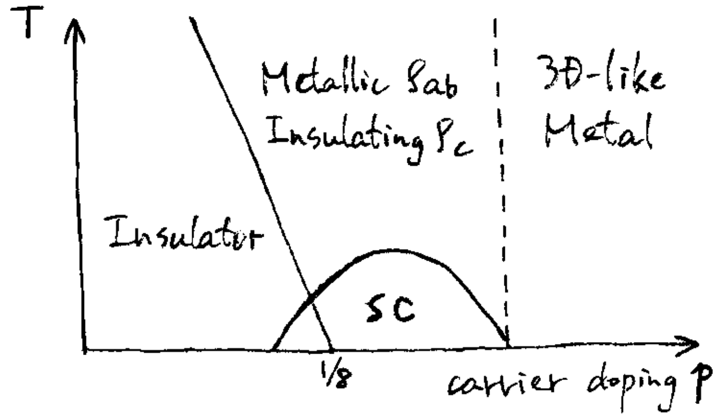

T
Metallic ρ_{ab}
Insulating ρ_c
3D-like
Metal
Insulator
SC
1/8
carrier doping p

LSCO and Bi-2201 … logT plot

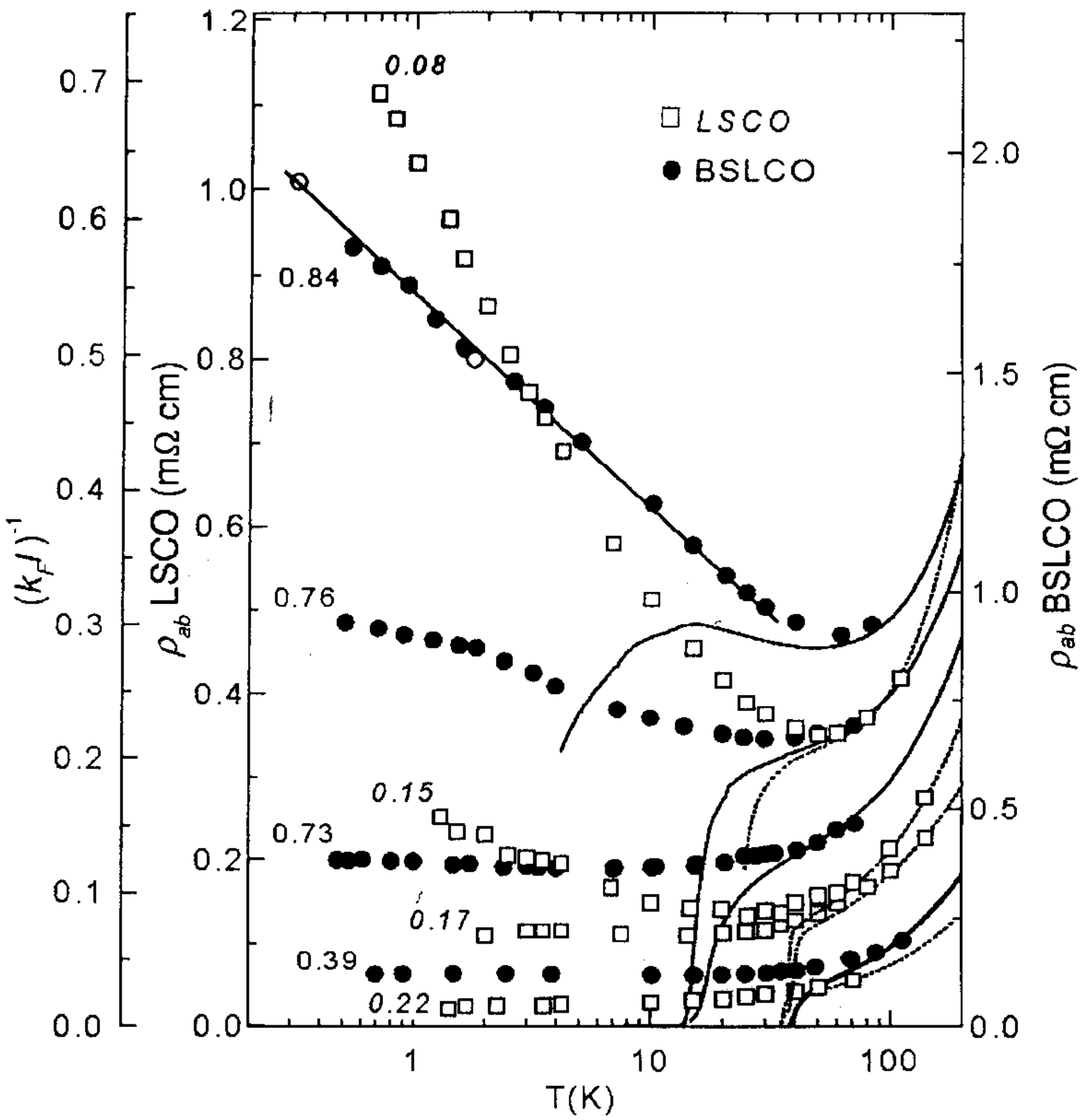

- Localization of the Luttinger liquid (Anderson)
- Impurity effect of Marginal Fermi liquid (Varma-Kotliar)
- Bipolaron localization (Alexandrov)

⋮

$La_{1.4-x}Nd_{0.6}Sr_xCuO_4$

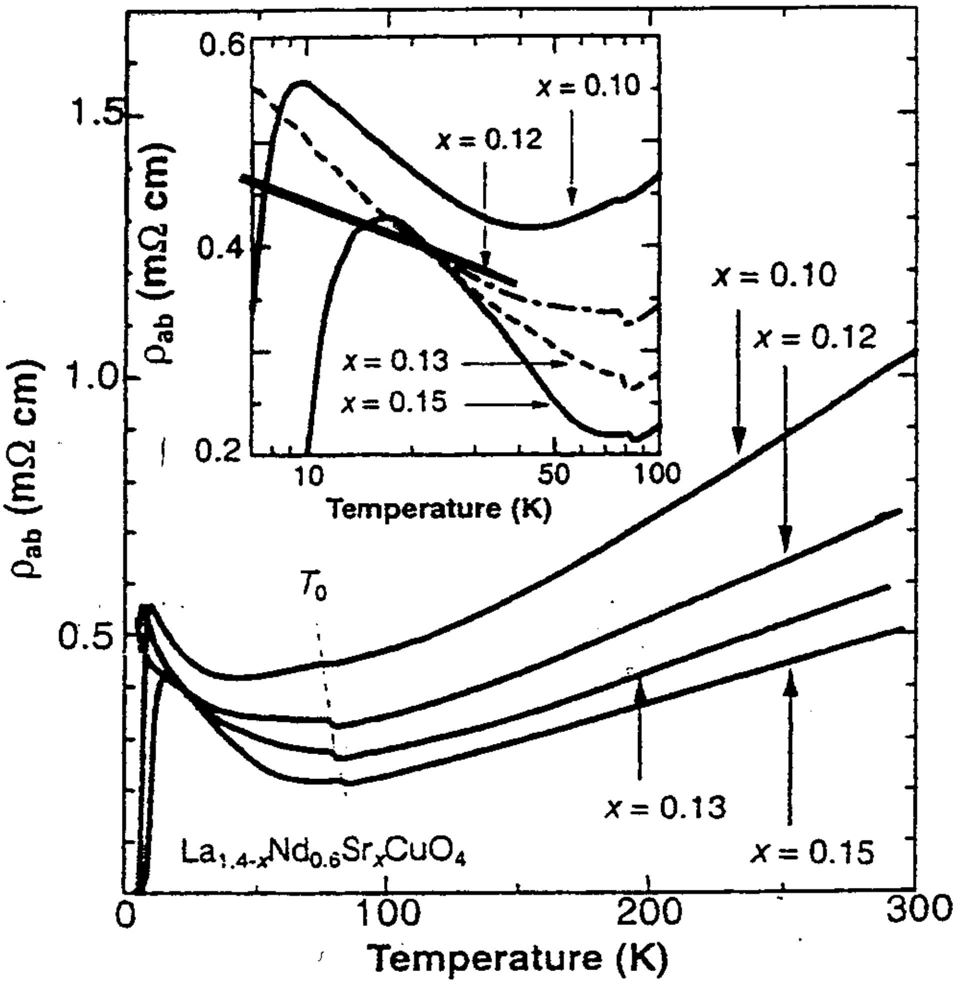

Fig. 1. Temperature dependence of in-plane resistivity (ρ_{ab}) of $La_{1.4-x}Nd_{0.6}Sr_xCuO_4$ with x = 0.10, 0.12, 0.13, and 0.15. **(Inset)** ρ_{ab} plotted on a logarithmic T scale. T_0 values of the samples are marked with a dashed line.

T. Noda et al., Science 286, 265 (1999).

Nature 375, 561 (1995)

Evidence for stripe correlations of spins and holes in copper oxide superconductors

J. M. Tranquada*, B. J. Sternlieb†, J. D. Axe*, Y. Nakamura† & S. Uchida†

* Physics Department, Brookhaven National Laboratory, Upton, New York 11973, USA

† Superconductivity Research Course, The University of Tokyo, Yayoi 2-11-16, Bunkyo-ku, Tokyo 113, Japan

ONE of the long-standing mysteries associated with the high-temperature copper oxide superconductors concerns the anomalous suppression[1] of superconductivity in $La_{2-x}Ba_xCuO_4$ (and certain related compounds) when the hole concentration x is near $\frac{1}{8}$. Here we examine the possibility that this effect is related to dynamical two-dimensional spin correlations, incommensurate with the crystal lattice, that have been observed in $La_{2-x}Sr_xCuO_4$ by neutron scattering[2-4]. A possible explanation for the incommensurability involves a coupled, dynamical modulation of spin and charge in which antiferromagnetic 'stripes' of copper spins are separated by periodically spaced domain walls to which the holes segregate[5-9]. An ordered stripe phase of this type has recently been observed in hole-doped La_2NiO_4 (refs 10–12). We present evidence from neutron diffraction that in the copper oxide material $La_{1.6-x}Nd_{0.4}Sr_xCuO_4$, with $x = 0.12$, a static analogue of the dynamical stripe phase is present, and is associated with an anomalous suppression of superconductivity[13,14]. Our results thus provide an explanation of the '$\frac{1}{8}$' conundrum, and also support the suggestion[15] that spatial modulations of spin and charge density are related to superconductivity in the copper oxides.

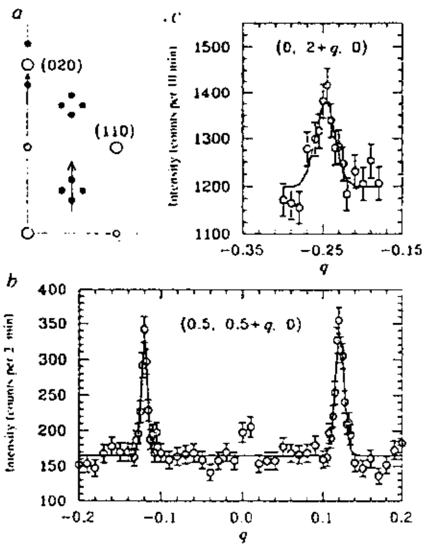

FIG. 3 Scans of superlattice peaks consistent with the proposed spin and charge stripes, in $La_{1.48}Nd_{0.4}Sr_{0.12}CuO_4$ at 11 K. *a*, Diagram of the (*hk*0) zone of reciprocal space. Open circles indicate locations of Bragg peaks for the LTT structure; solid circles denote spin- and charge-ordering superlattice peaks. Arrows indicate the regions scanned. *b*, Scan along $(\frac{1}{2}, \frac{1}{2}+q, 0)$ through the $(\frac{1}{2}, \frac{1}{2}\pm\epsilon, 0)$ peaks measured with a neutron energy of 13.9 meV. The small peak width indicates that the in-plane correlation length is greater than 150 Å. *c*, Scan along $(0, 2+q, 0)$ through the $(0, 2-2\epsilon, 0)$ peak using 14.7-meV neutrons. The lines in *b* and *c* are the result of least-squares fits to gaussian peak shapes plus a flat background.

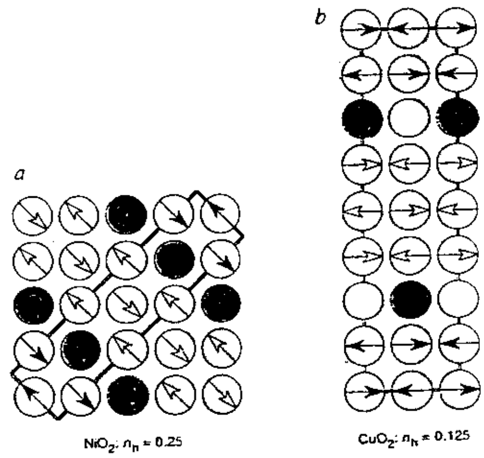

FIG. 1 *a*, Idealized diagram of the spin and charge stripe pattern within a NiO_2 plane observed in hole-doped La_2NiO_4 with a hole density of $n_h = \frac{1}{4}$. *b*, Hypothesized stripe pattern in a CuO_2 plane of hole-doped La_2CuO_4 with $n_h = \frac{1}{8}$. In both, only the metal atoms are represented; the oxygen atoms, which surround the metal sites in a square planar array (as shown in Fig. 2), have been omitted. Arrows indicate the orientation of magnetic moments on metal atoms, which are locally antiparallel; the spin direction rotates by 180° (relative to a simple antiferromagnetic structure) on crossing a domain wall, as emphasized by the change in filling of the arrow heads. The doubled lines outline the magnetic unit cell in each case. Holes are located at the anti-phase domain boundaries, which are indicated by the rows of circles without arrows. A filled circle denotes the presence of one hole, centred on a metal site. For the present analysis, the hole density is assumed to be uniform along a domain wall; the ordering of holes along stripes suggested in *b* has not been tested experimentally, but serves as a reminder that the hole per Cu ratio is $\frac{1}{8}$.

$La_{2-x}Sr_xCuO_4$

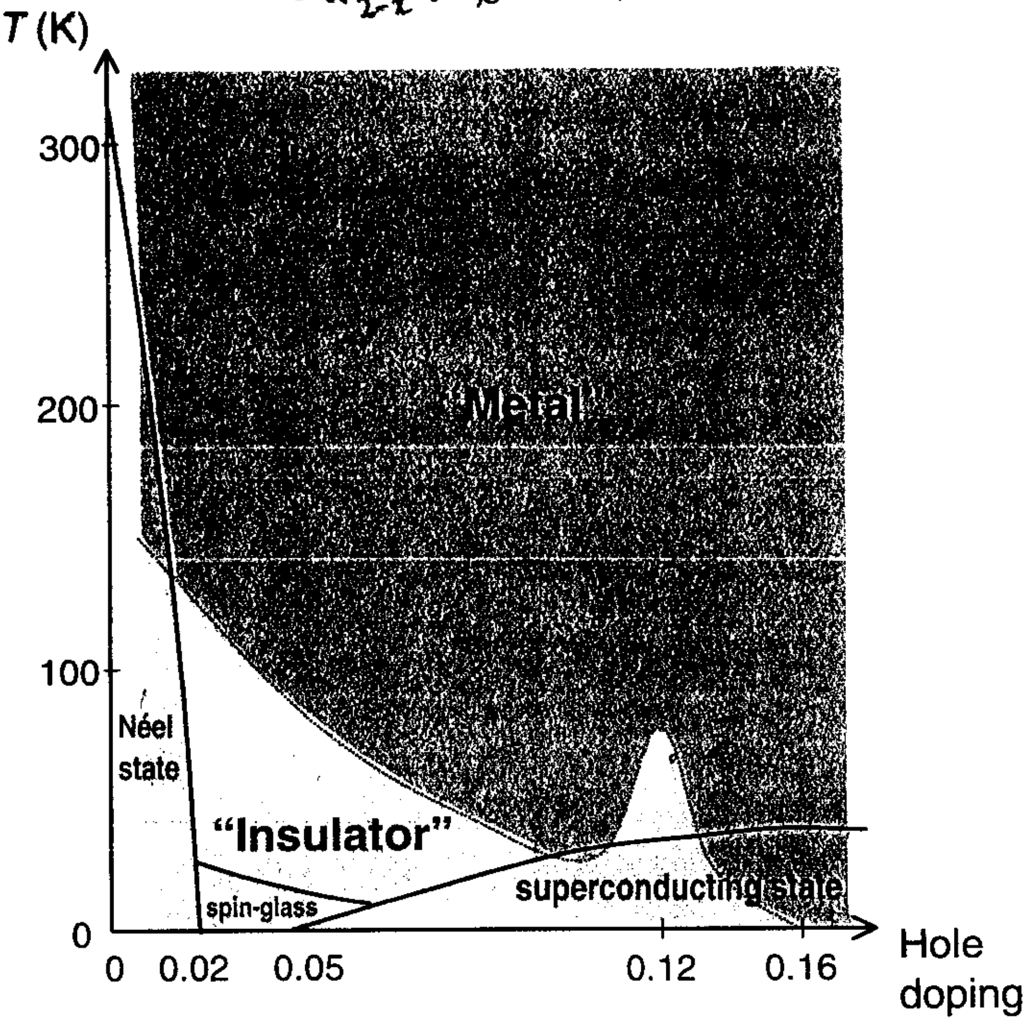

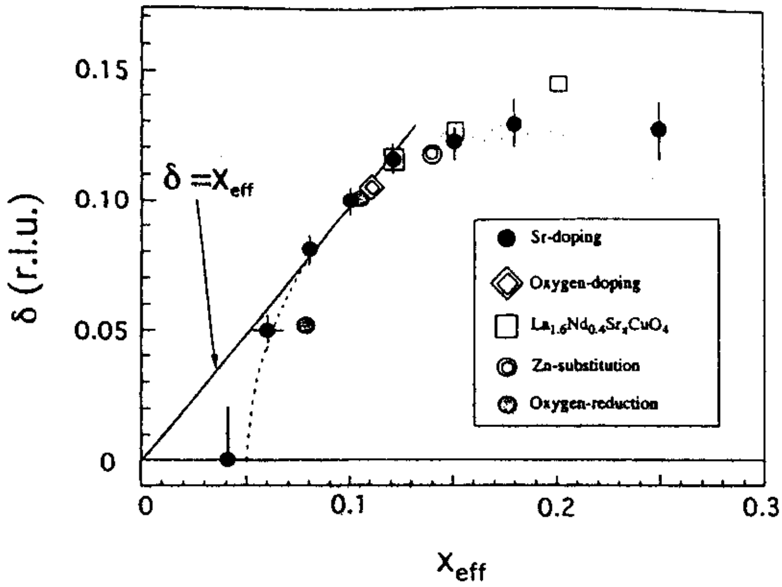

FIG. 7. Sr-doping dependence of the incommensurability δ of the spin fluctuations. The height of the vertical bar at $x=0.04$ indicates the upper limit of δ estimated from the single peaked spectrum in Fig. 5. Data from electrochemically oxygen-doped La_2CuO_{4+y} (Ref. 6), $La_{1.6}Nd_{0.4}Sr_xCuO_4$ (Ref. 38), Zn-substituted $La_{1.86}Sr_{0.14}Cu_{1-y}Zn_yO_4$ with $y=0.012$ (Ref. 22) and deoxygenated $La_{1.85}Sr_{0.15}CuO_{4-y}$ (see Fig. 8) are also plotted in the figure.

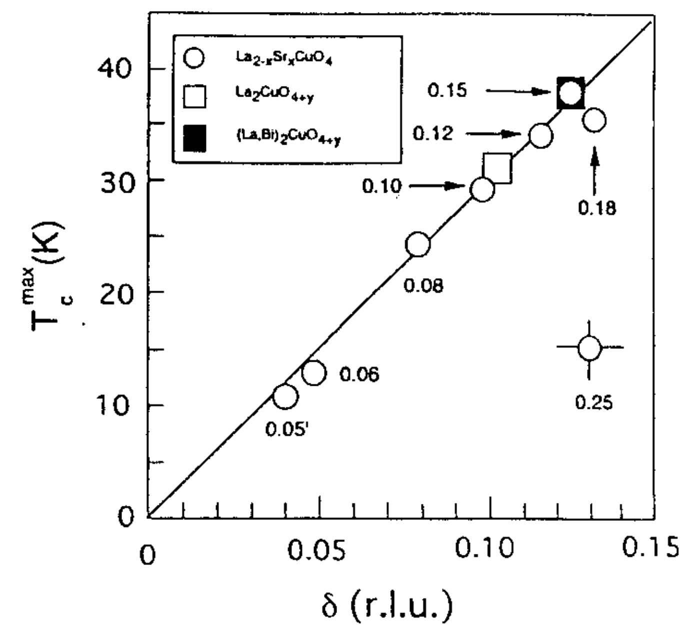

FIG. 10. δ as a function of onset temperature of T_c for stoichiometric $La_{2-x}Sr_xCuO_4$ (open circles), electrochemically oxygen-doped La_2CuO_{4+y} (Ref. 6) (open square) or $(La,Bi)_2CuO_{4+y}$ (Ref. 32) (closed square), and $La_{1.95}Sr_{0.05}CuO_4$ annealed under high O_2 pressure (Ref. 32) (closed circle).

K. Yamada et al.
PRB 57, 6165 ('98)

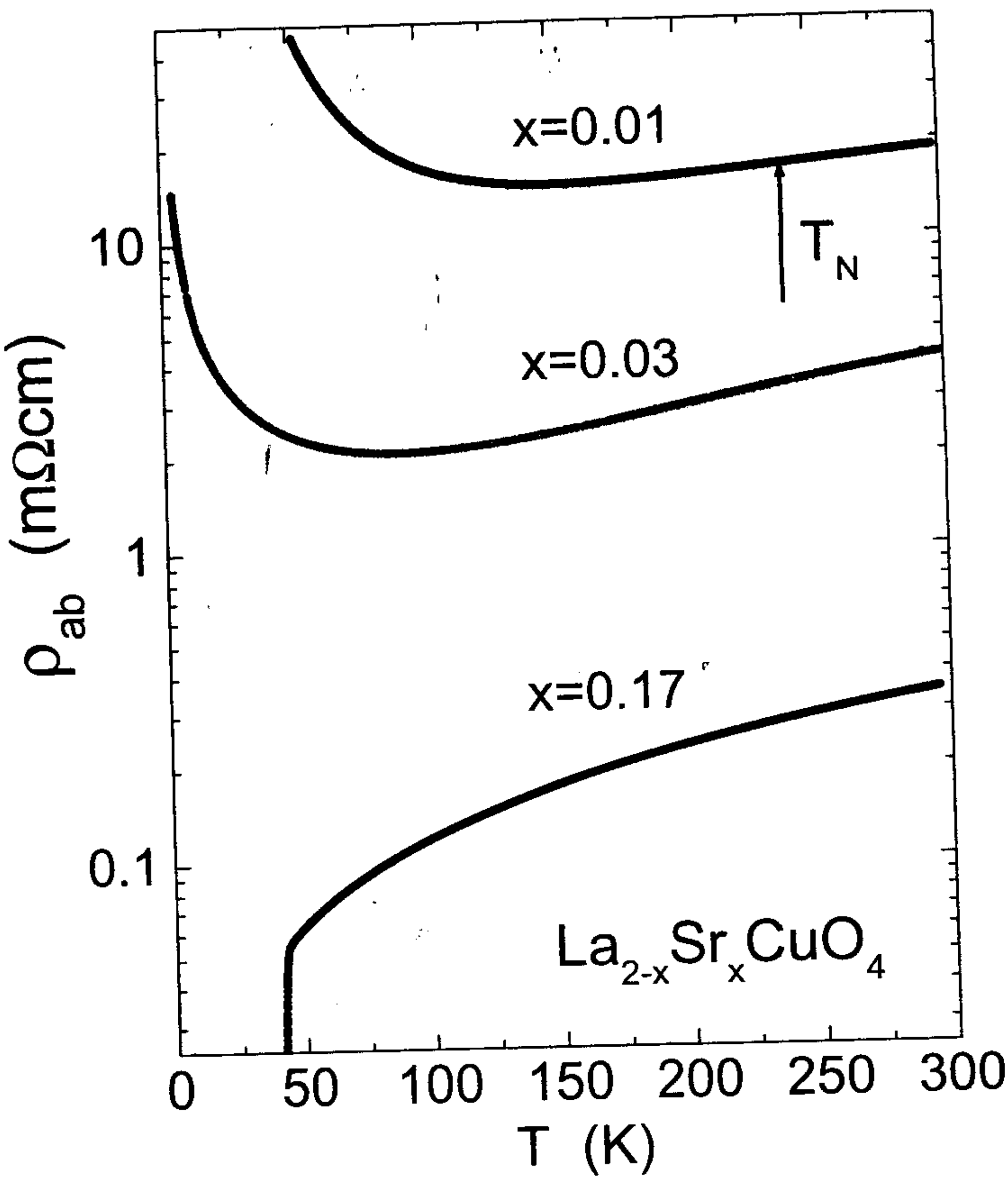

x=0.01
T_N
x=0.03
x=0.17
$La_{2-x}Sr_xCuO_4$
10
1
0.1
ρ_{ab} (mΩcm)
0
50
100
150
200
250
300
T (K)

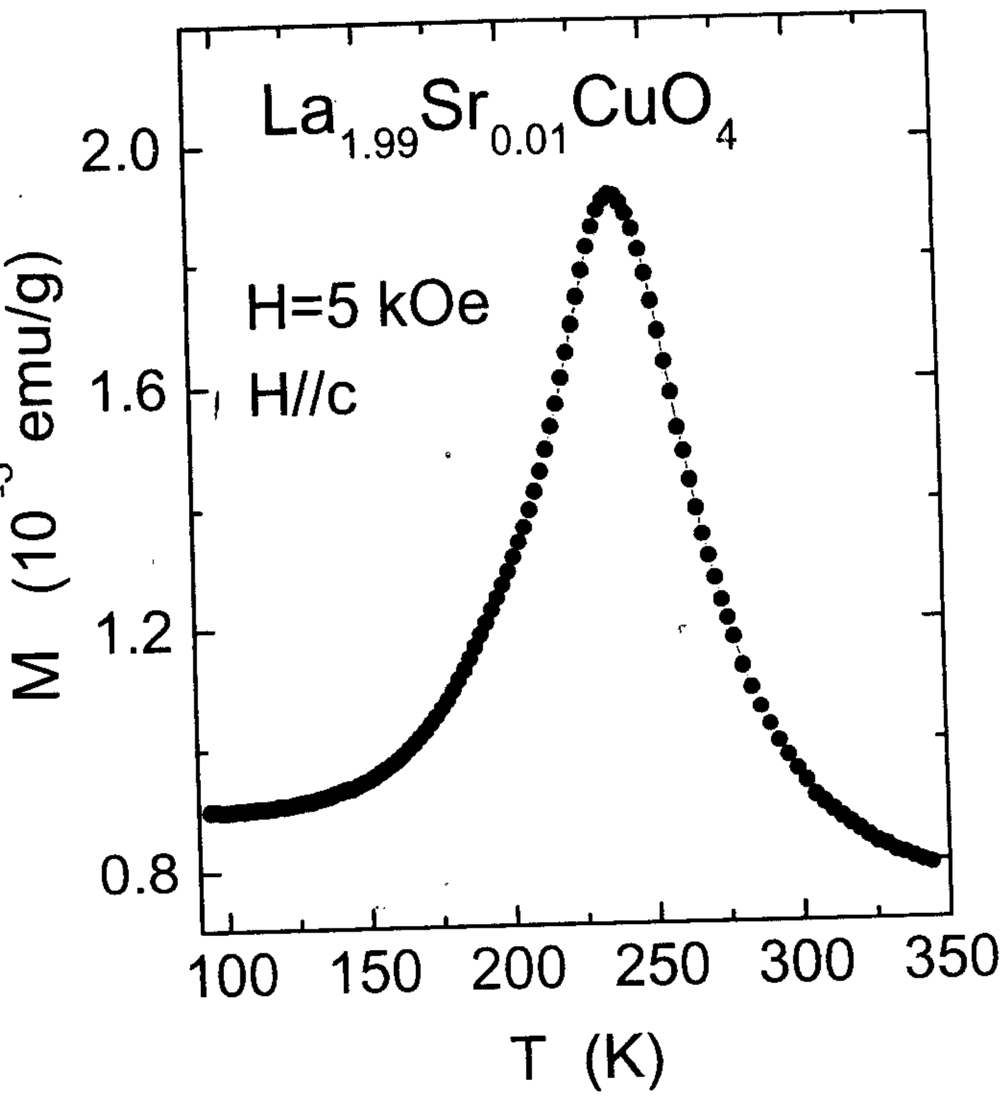
La1.99Sr0.01CuO4
H=5 kOe
H//c
M (10-3 emu/g)
2.0
1.6
1.2
0.8
100
150
200
250
300
350
T (K)

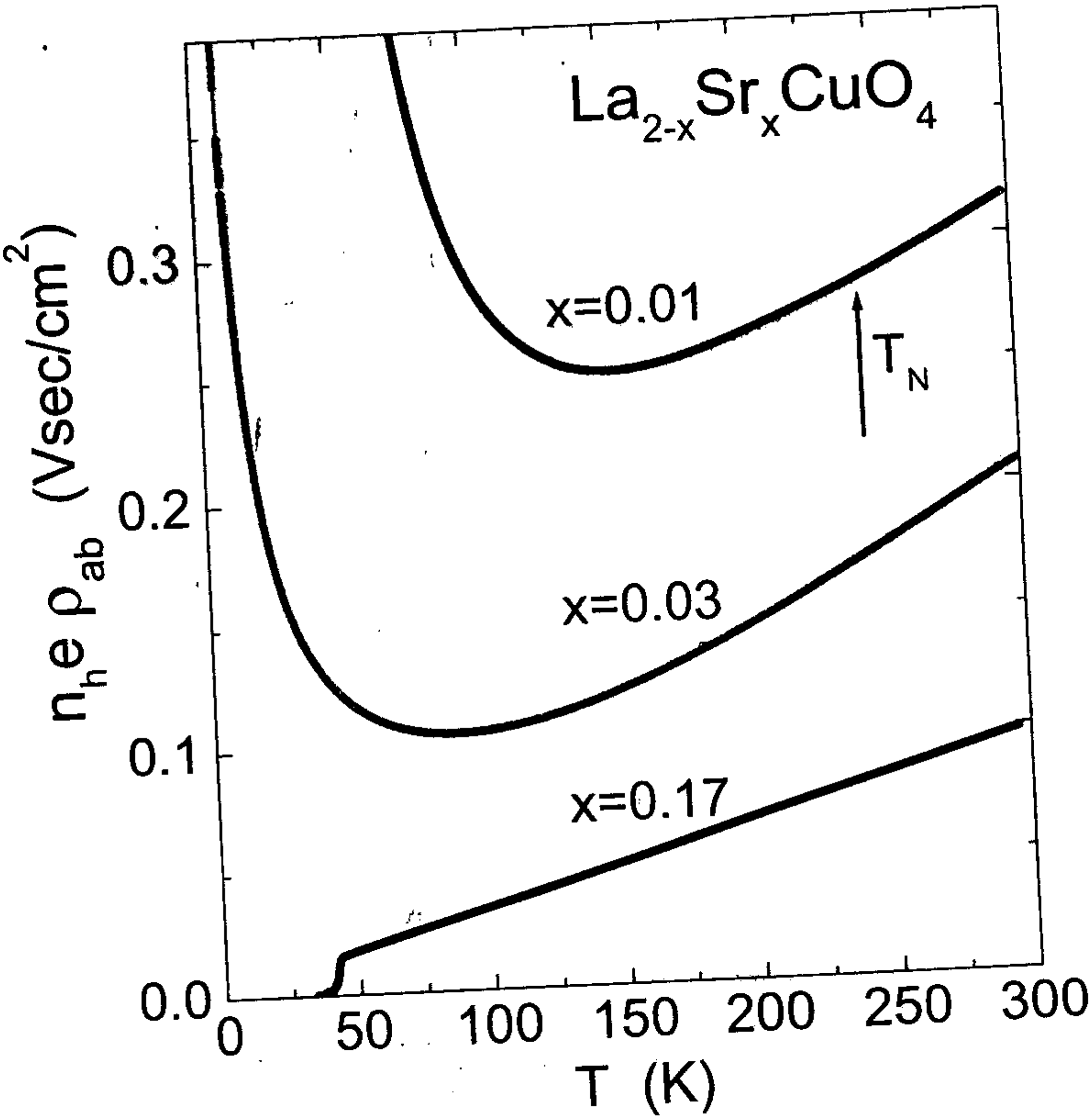

mobility $\mu = \sigma_{ab} \cdot R_H = \frac{ne^2\tau}{m^*} \cdot \frac{1}{ne} = \frac{\tau e}{m^*}$

$$= \frac{1}{ne\rho_{ab}}$$

$$\therefore\ n_h e \rho_{ab} \leftrightarrow \mu^{-1} \left(\propto \frac{m^*}{\tau}\right)$$

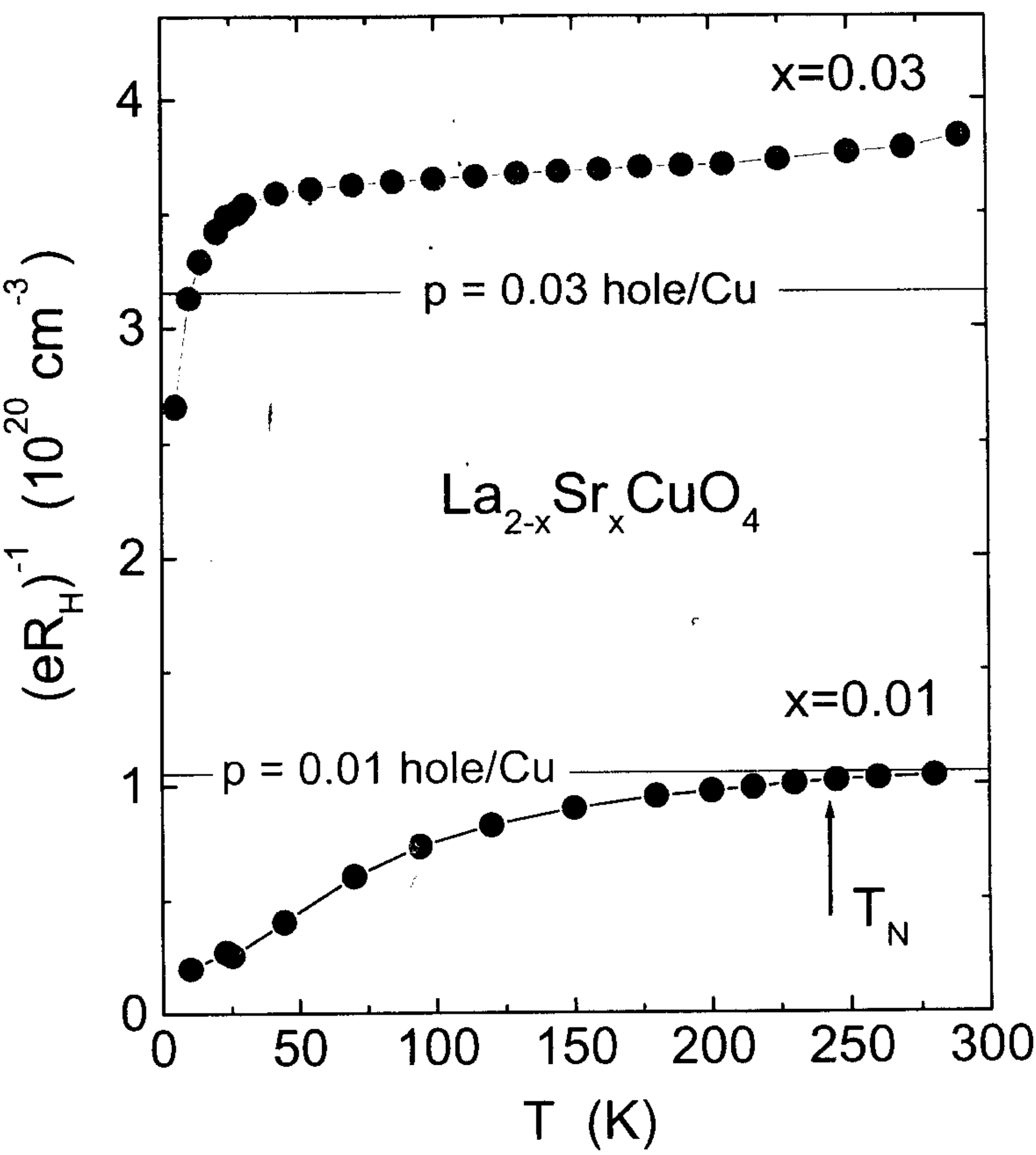
x=0.03
p = 0.03 hole/Cu
$La_{2-x}Sr_xCuO_4$
x=0.01
p = 0.01 hole/Cu
T_N
$(eR_H)^{-1}$ $(10^{20}$ $cm^{-3})$
T (K)
0
50
100
150
200
250
300
1
2
3
4

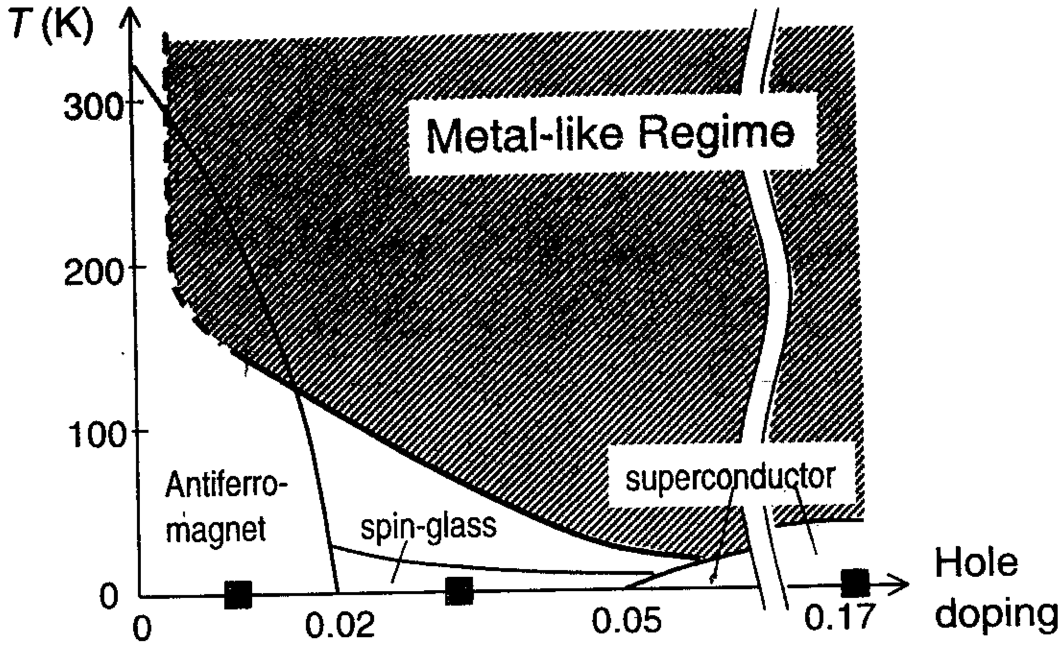

T (K)
300
200
100
0
Metal-like Regime
Antiferro-
magnet
spin-glass
superconductor
0
0.02
0.05
0.17
Hole
doping

Motion of a single hole

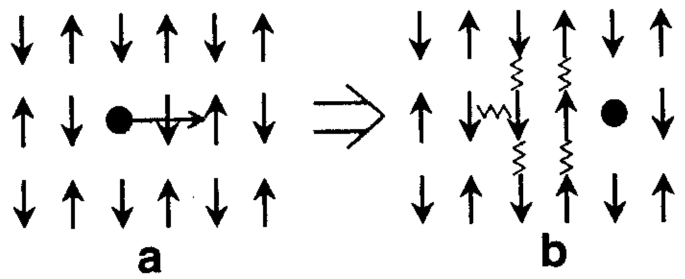

: frustrated bond

Motion of a charged stripe (anti-phase boundary)

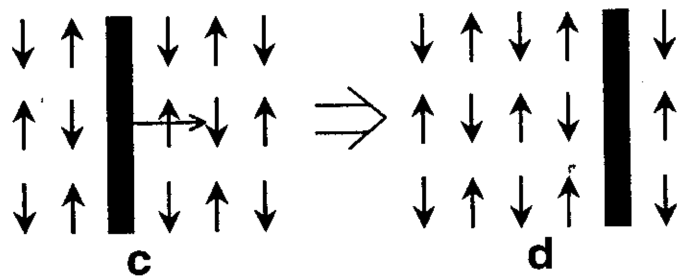

long-range order
is destroyed

Motion of a double-raw stripe (in-phase boundary)

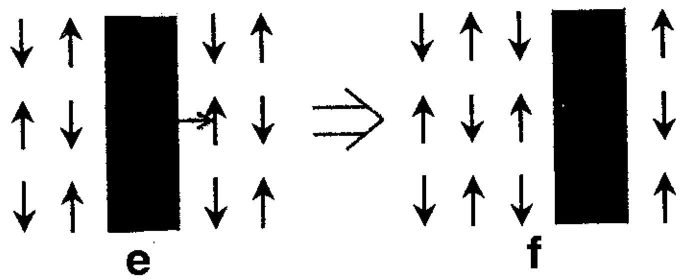

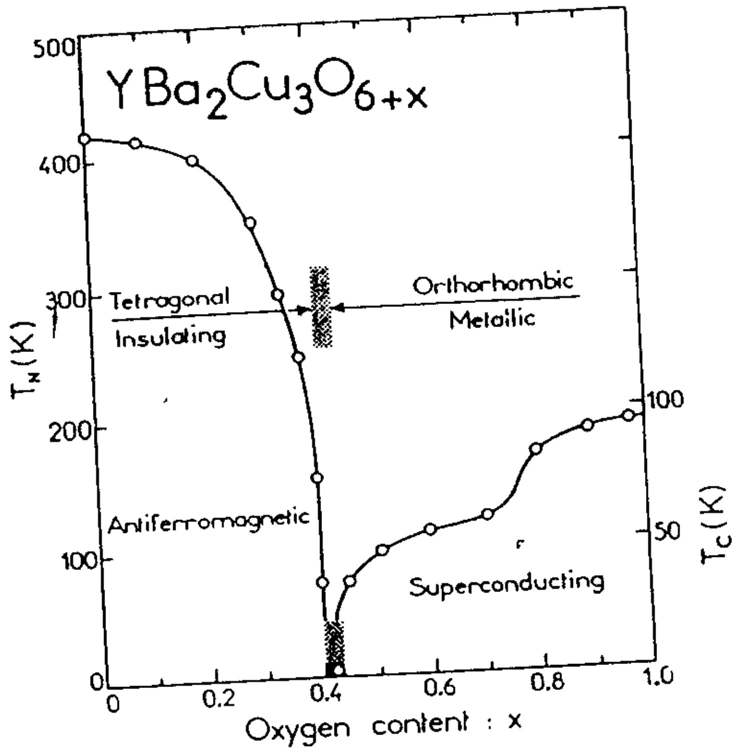

Fig. 1. Phase diagram of the $YBaCu_3O_{6+x}$ system as a function of the oxygen content.

J. Rossat-Mignod et al. Physica B 169, 58 (1991).

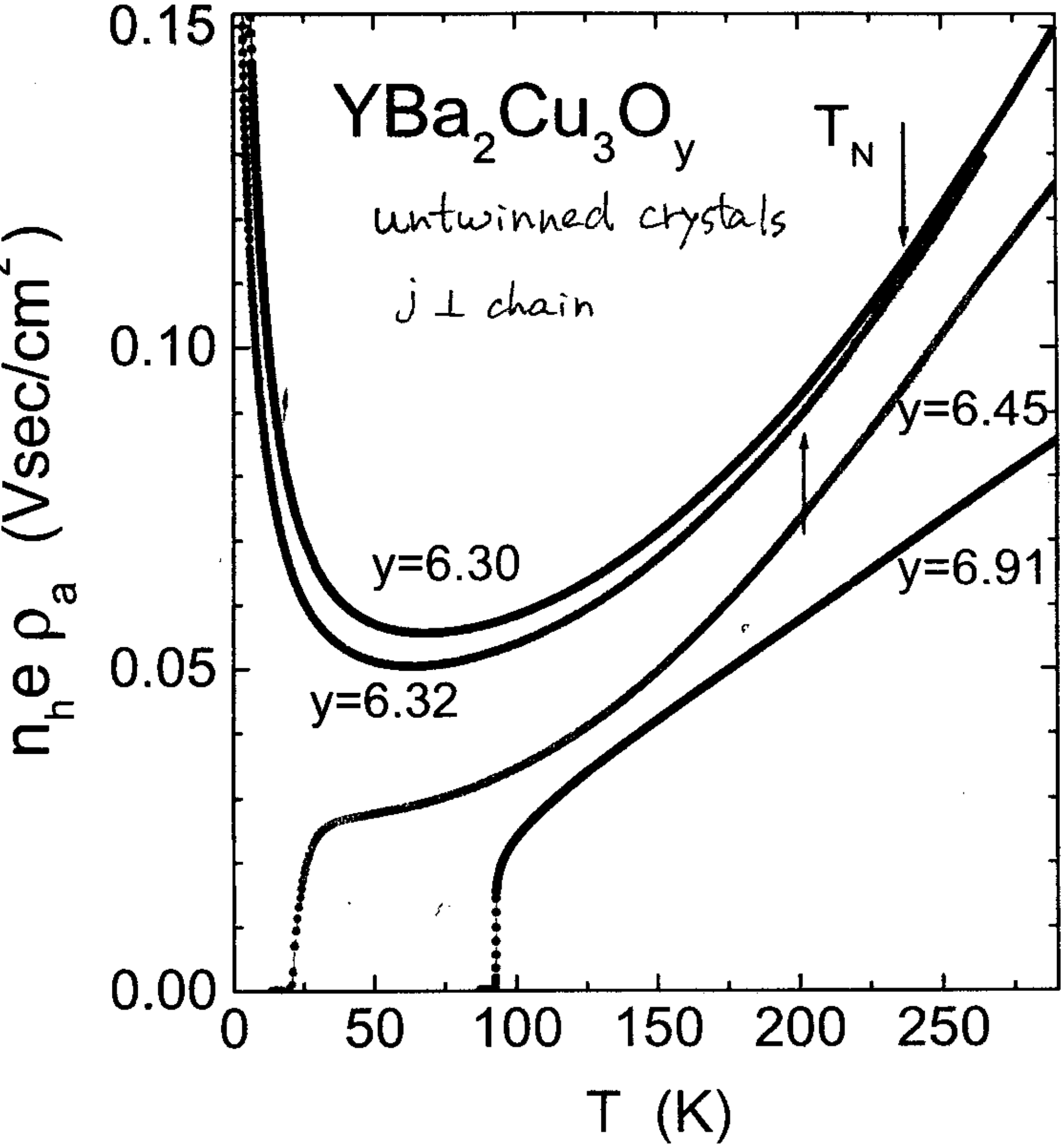

$n_h e \rho_a = \mu^{-1} = \frac{m^*}{\tau}$

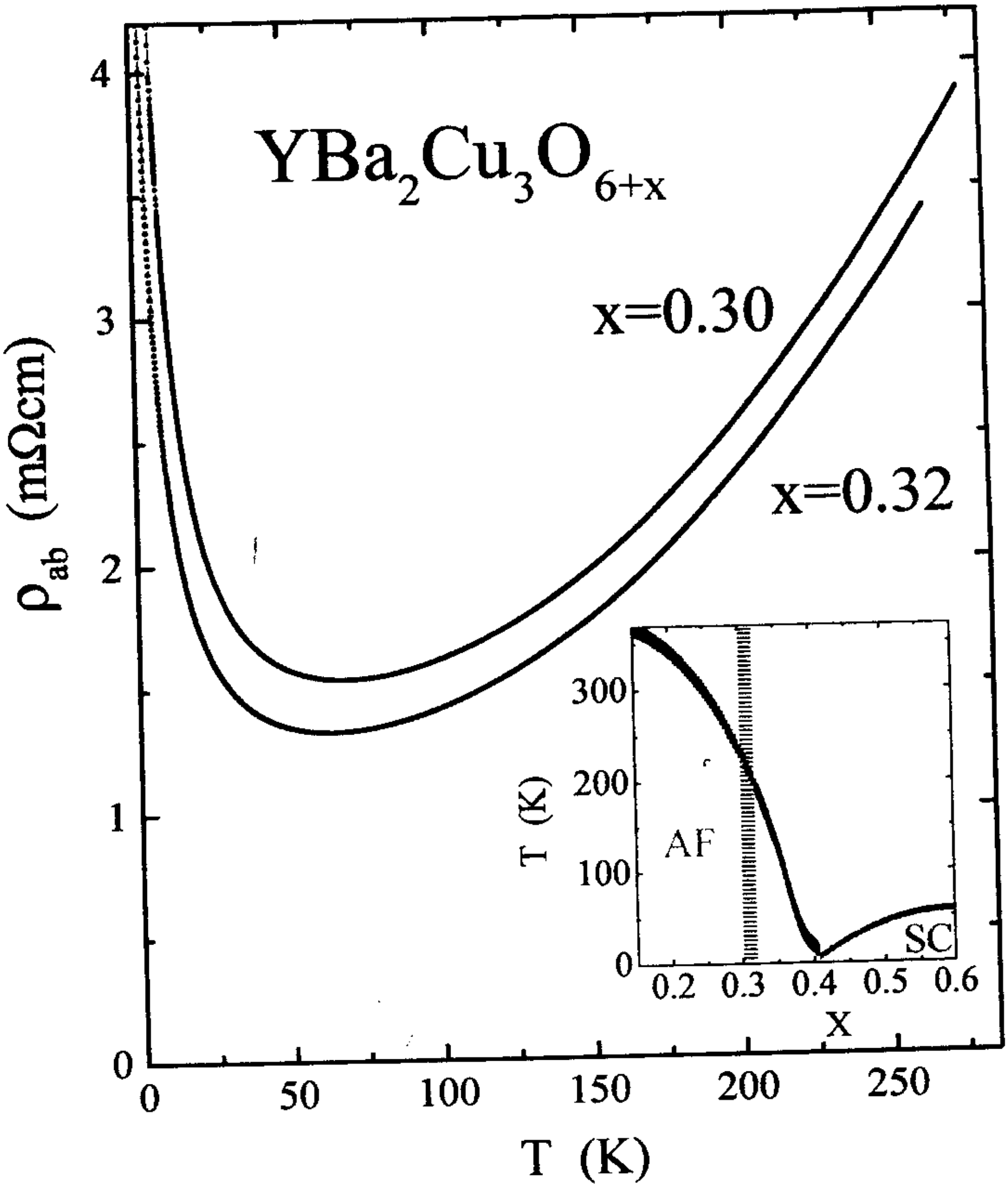
YBa2Cu3O6+x
x=0.30
x=0.32
ρab (mΩcm)
T (K)
0
1
2
3
4
0
50
100
150
200
250
T (K)
300
200
100
0
AF
SC
0.2
0.3
0.4
0.5
0.6
X

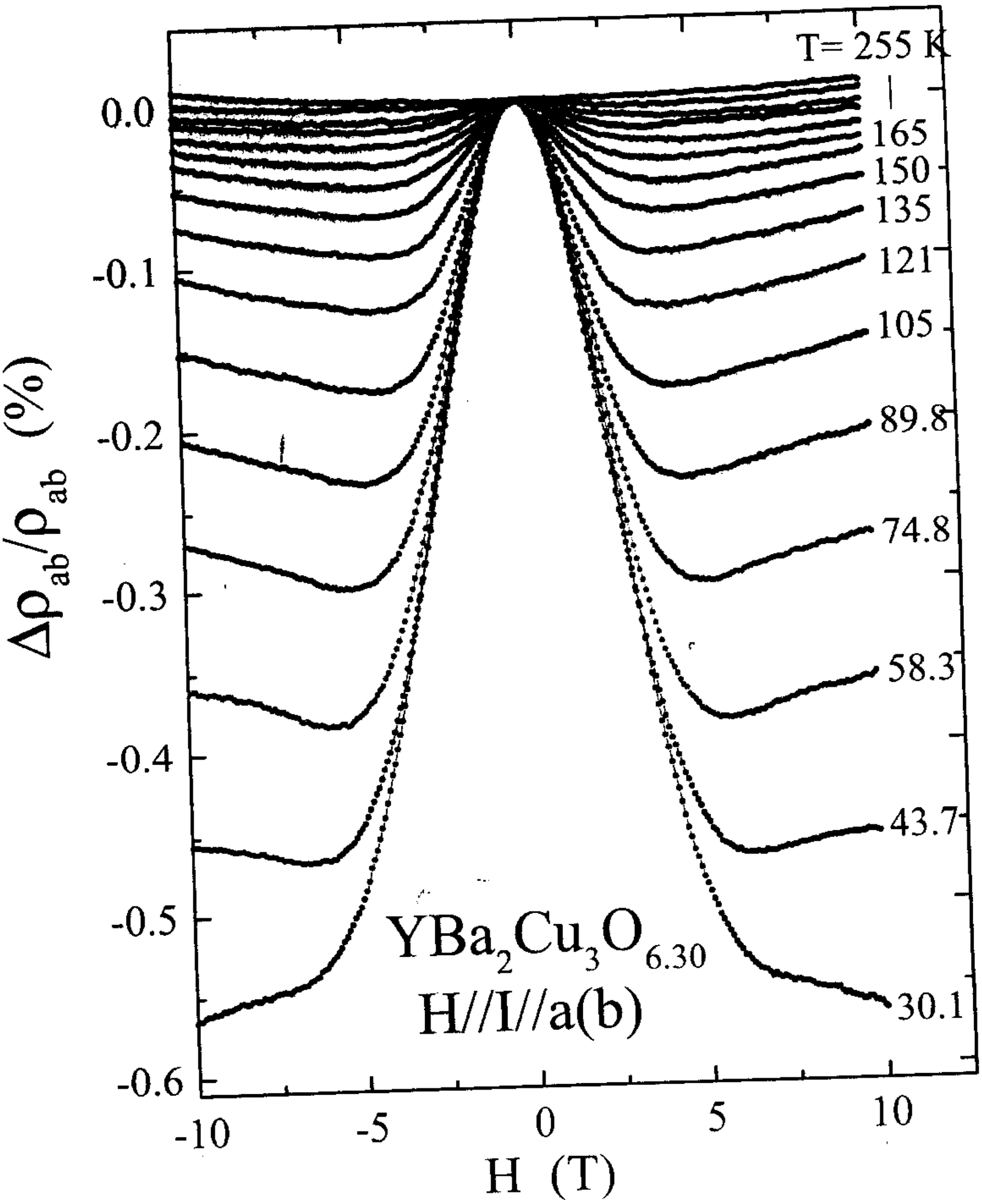

T= 255 K
165
150
135
121
105
89.8
74.8
58.3
43.7
30.1
0.0
-0.1
-0.2
-0.3
-0.4
-0.5
-0.6
$\Delta\rho_{ab}/\rho_{ab}$ (%)
-10
-5
0
5
10
H (T)
$YBa_2Cu_3O_{6.30}$
H//I//a(b)

$YBa_2Cu_3O_{6.3}$

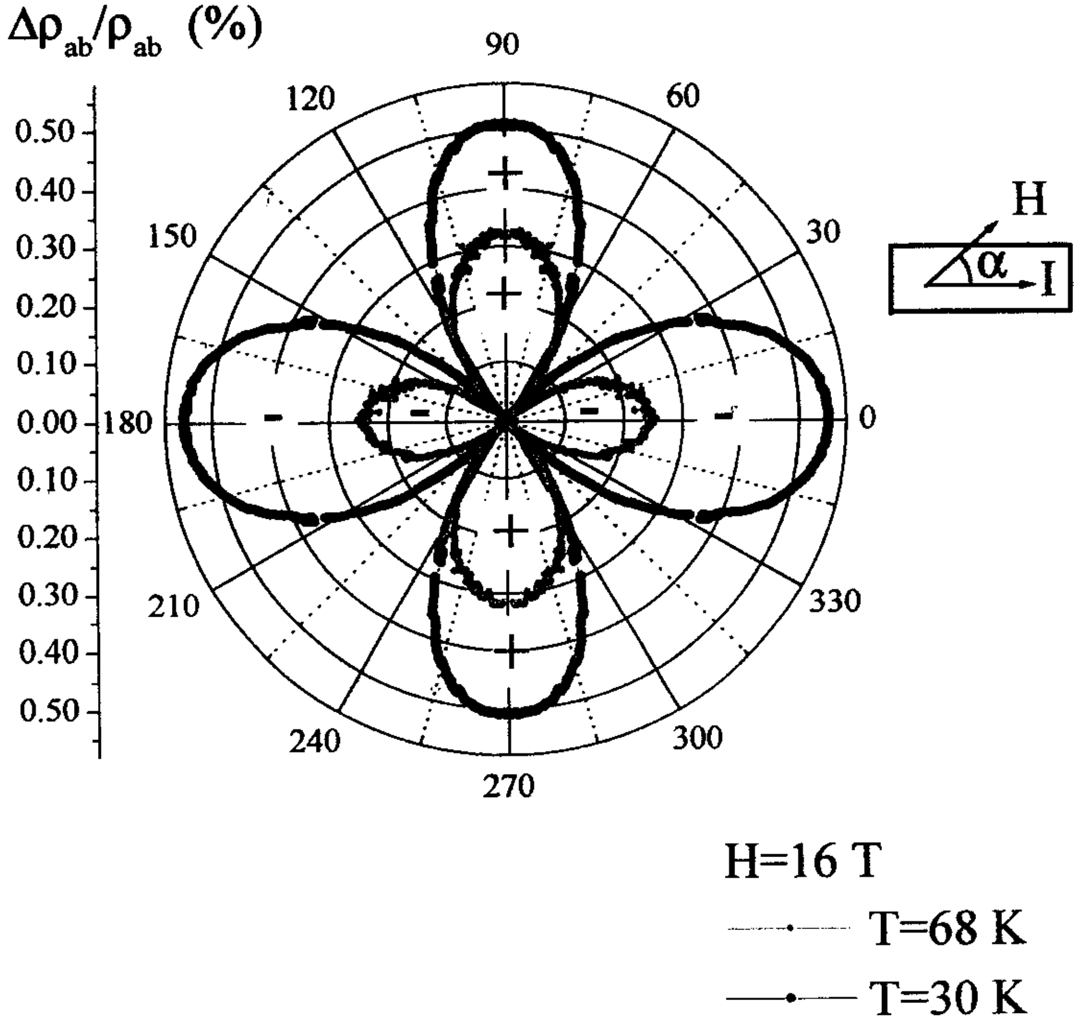

Δρab/ρab (%)
0.50
0.40
0.30
0.20
0.10
0.00
0.10
0.20
0.30
0.40
0.50
90
120
60
150
30
180
0
210
330
240
300
270
+
+
+
+
-
-
-
-
H
α
I
H=16 T
T=68 K
T=30 K

Suppose the stripes make the "Rivers of Charges":

Decrease in ρ_{ab}

→ Easier current flow

→ I must be parallel to the stripes

Increase in ρ_{ab}

→ More difficult current flow

→ I must be perpendicular to the stripes

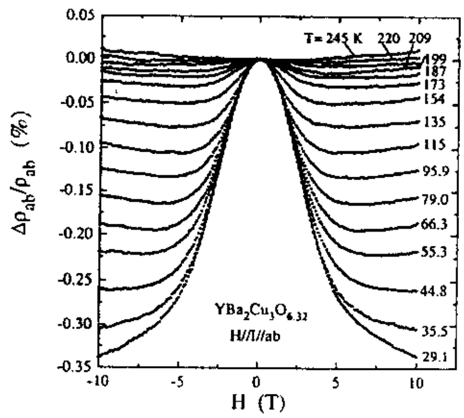

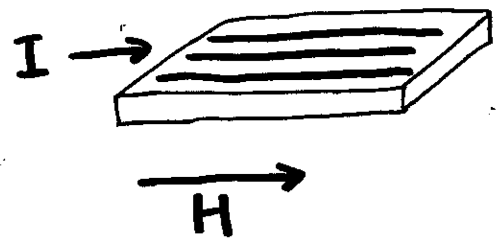

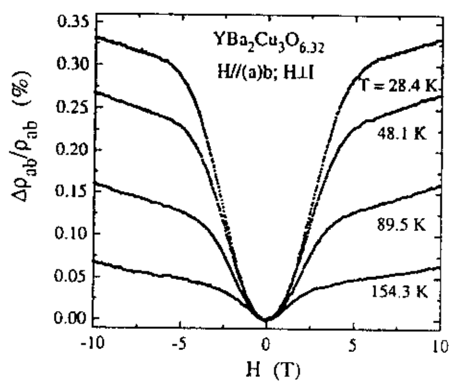

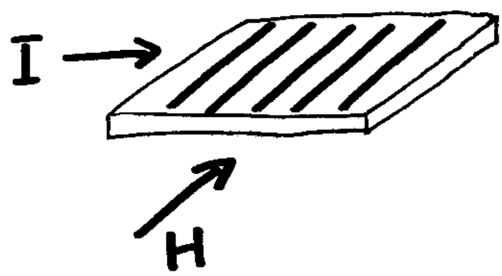

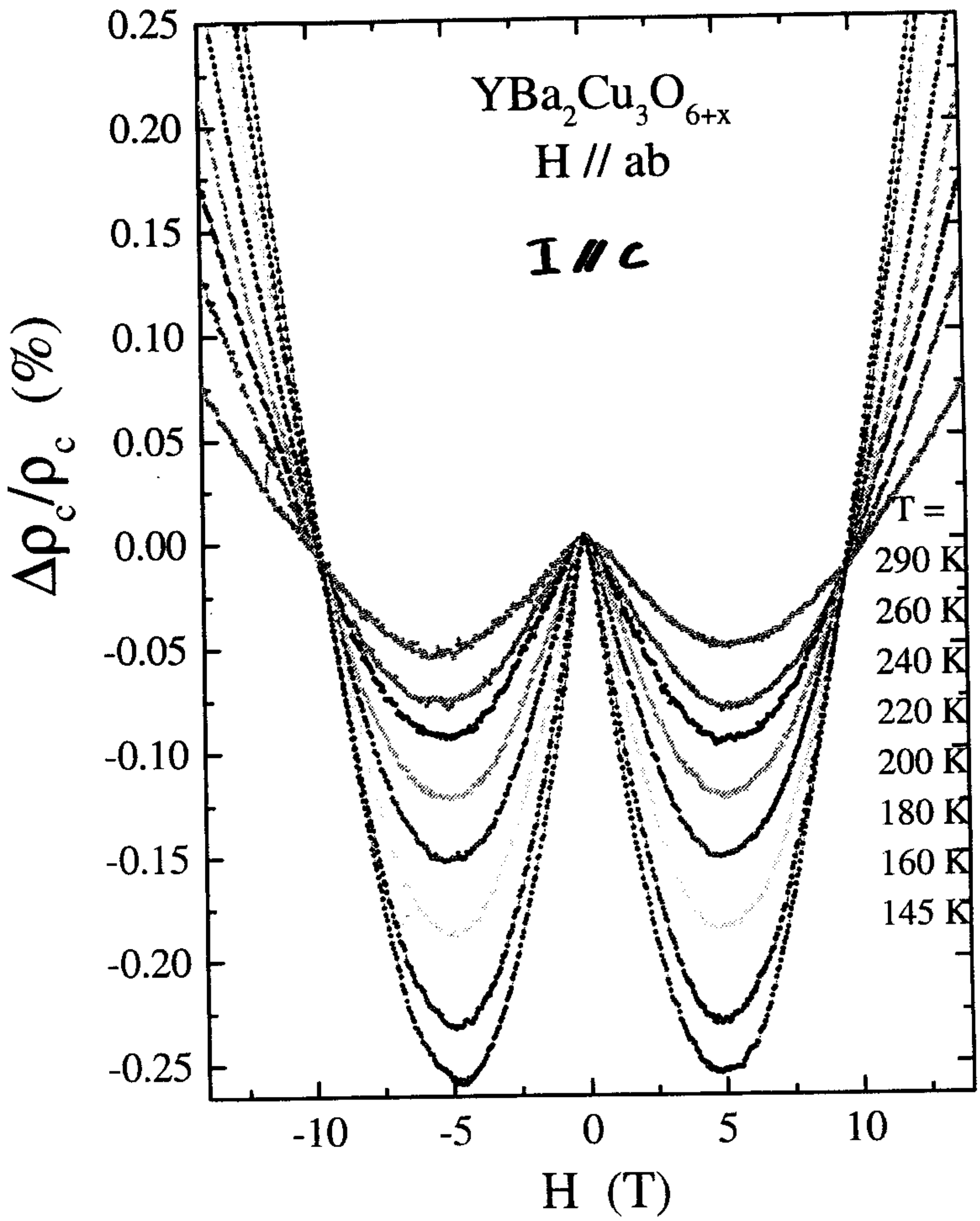
YBa2Cu3O6+x
H // ab
I // c
Δρc/ρc (%)
H (T)
T =
290 K
260 K
240 K
220 K
200 K
180 K
160 K
145 K
0.25
0.20
0.15
0.10
0.05
0.00
-0.05
-0.10
-0.15
-0.20
-0.25
-10
-5
0
5
10

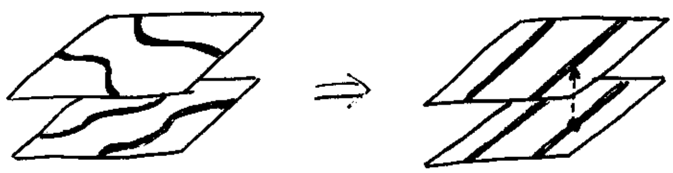

Possibilities for the A.F. YBCO with doped holes

A.

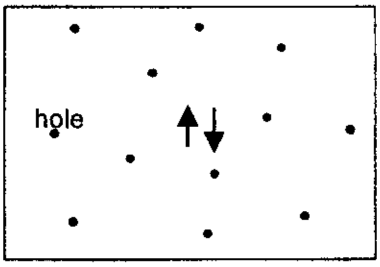

Single Domain AF

All the spins lie along one of the easy axes
(*a* and *b* axes are not equivalent)

B.

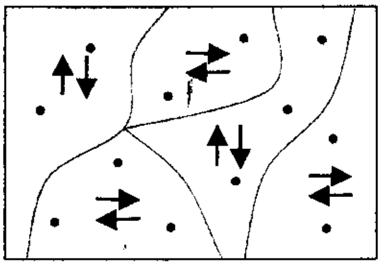

AF domain structure

a and *b* axes are equivalent

Domain walls have a large energy cost

~ NJ (N: number of broken bonds)

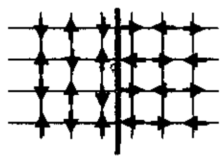

C.

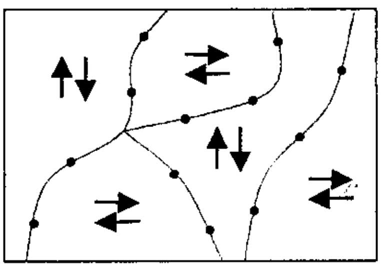

AF domain structure with charged stripes

Charges are confined in the domain walls

Energy cost of the domain walls are smaller than the case B.

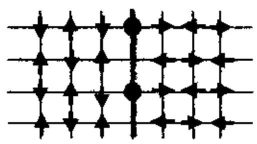

D.

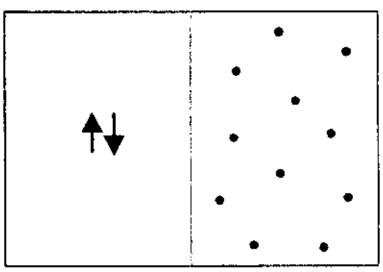

Macroscopic phase separation

Charged regions must be SC, if they are not AF.

In large magnetic field, sublattice magnetizations are oriented perpendicular to the field direction.
(ESR results by Janossy *et al.*, PRB 59, 1176 [1999].)

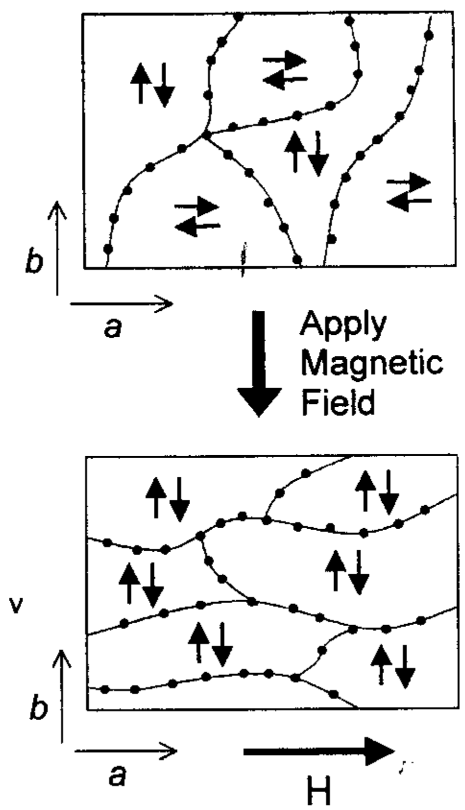

Zero-field

Equal population of M_s along *a* and *b*

High Field (above 5 T)

All the domains have M_s along *b*

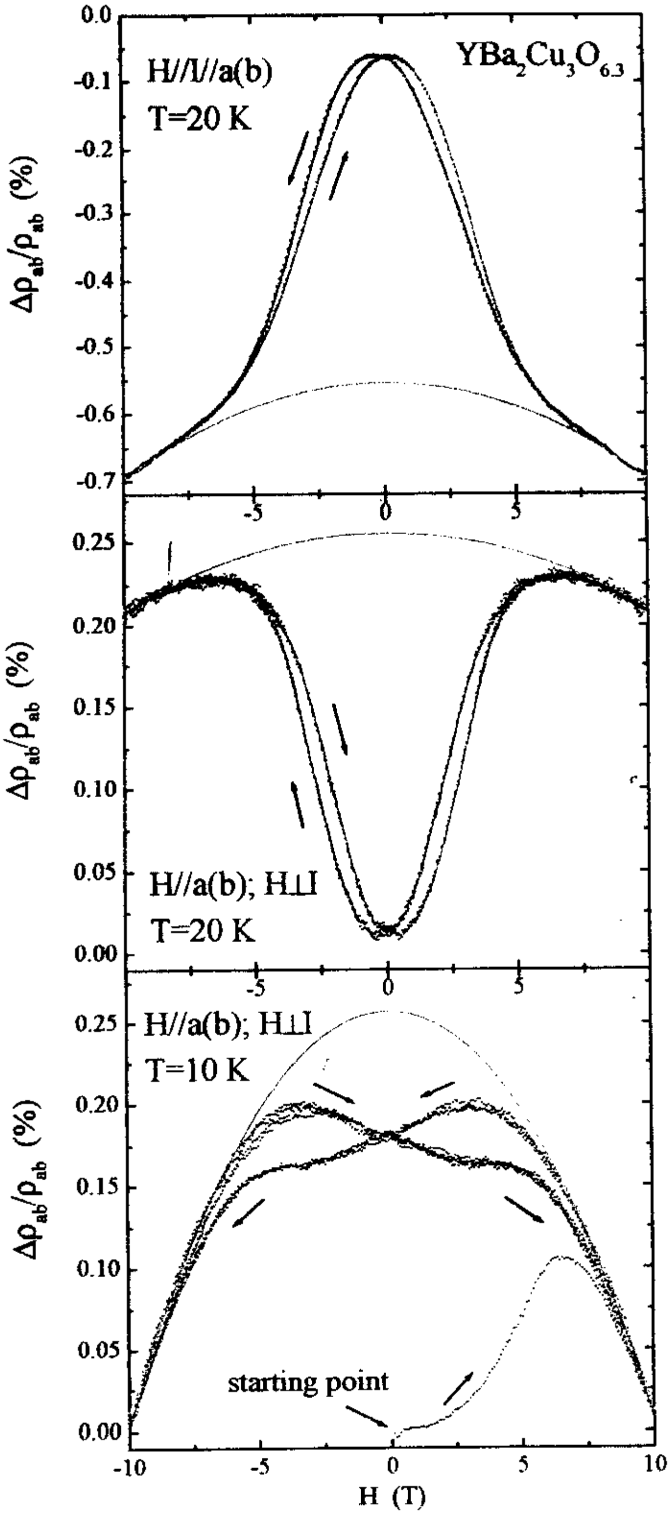
YBa2Cu3O6.3
H//I//a(b)
T=20 K
H//a(b); H⊥I
T=20 K
H//a(b); H⊥I
T=10 K
starting point
Δρab/ρab (%)
H (T)

Nd-doped LSCO, x=0.12
($La_{1.28}Nd_{0.6}Sr_{0.12}CuO_4$)
H // c, I // [110]
(Current is along 45 deg. direction)

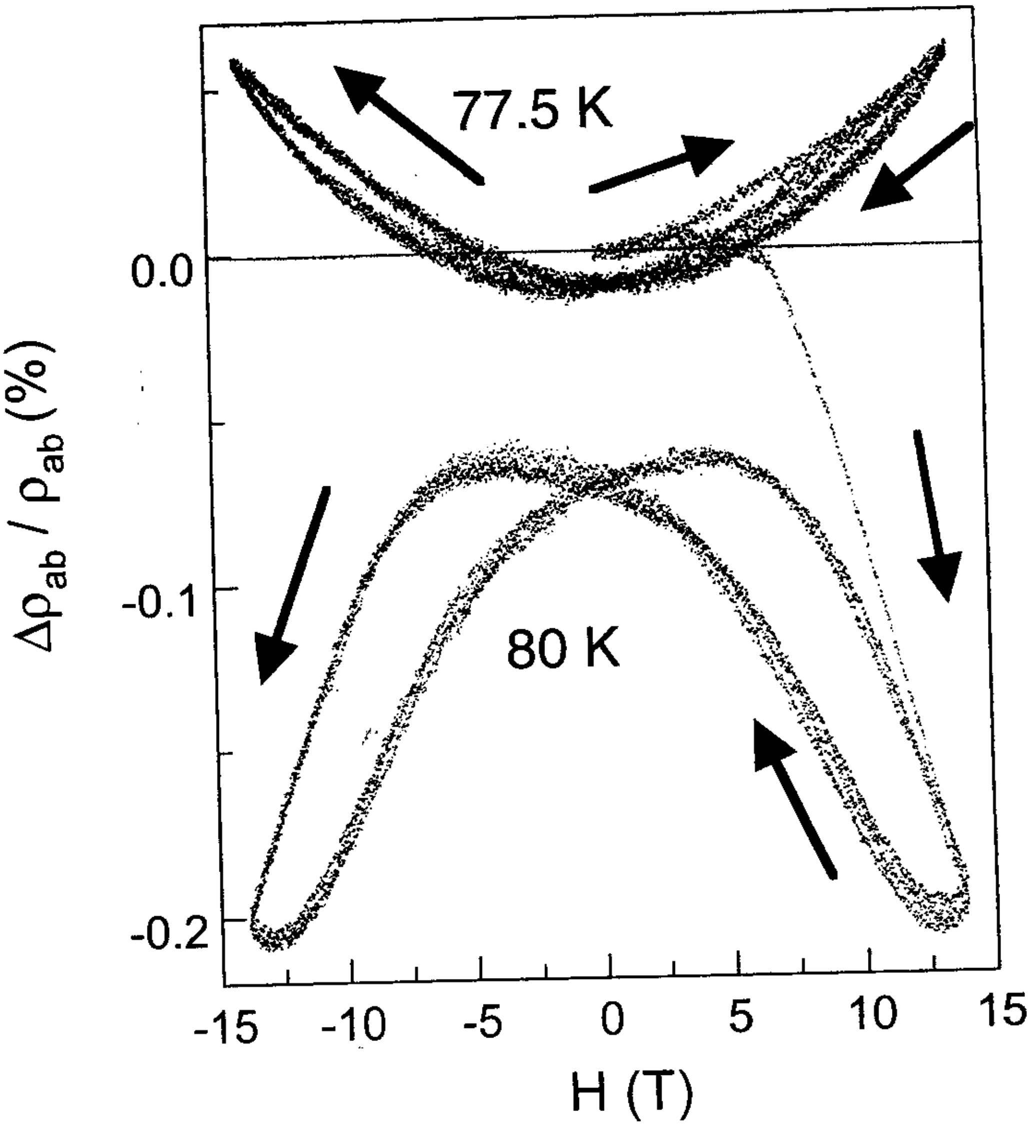

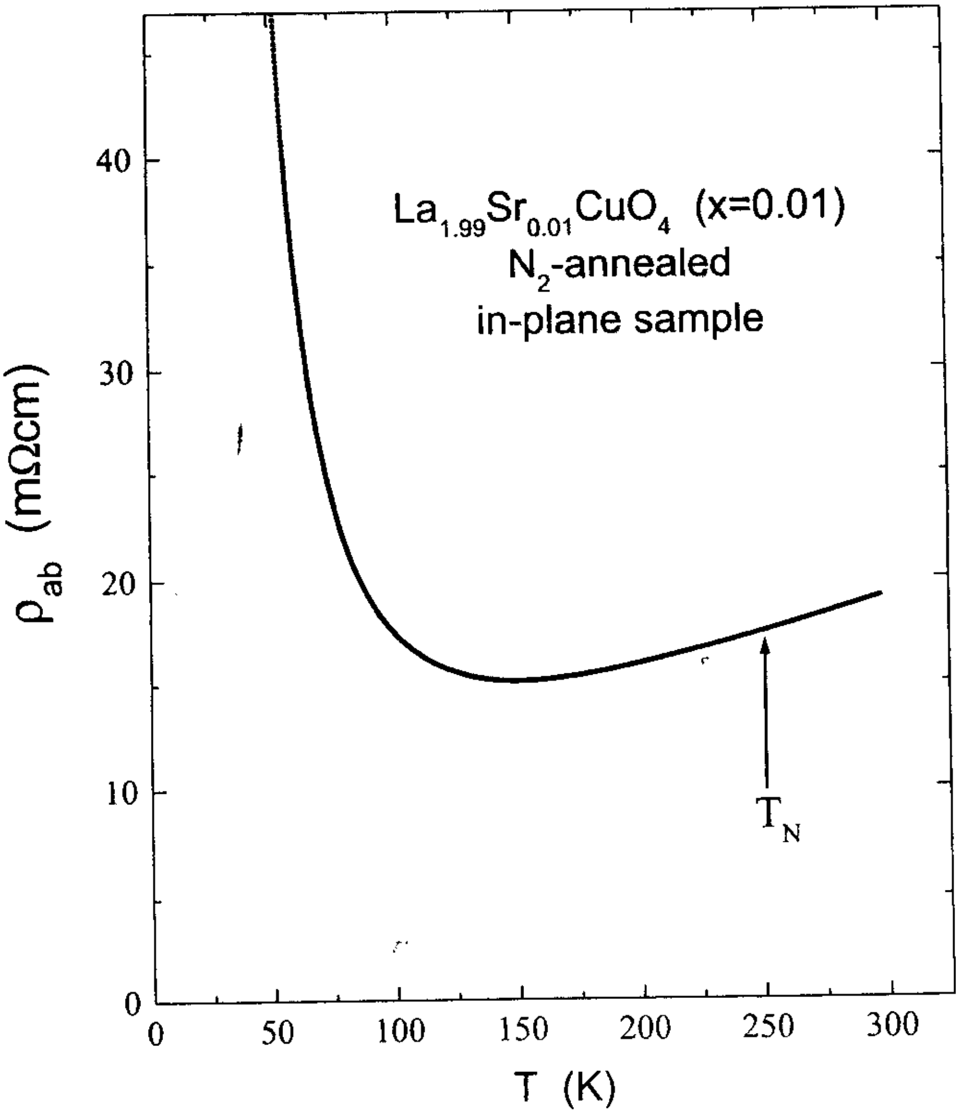

$La_{1.99}Sr_{0.01}CuO_4$ (x=0.01)
N_2-annealed
in-plane sample
T_N
ρ_{ab} (mΩcm)
T (K)
0
10
20
30
40
0
50
100
150
200
250
300

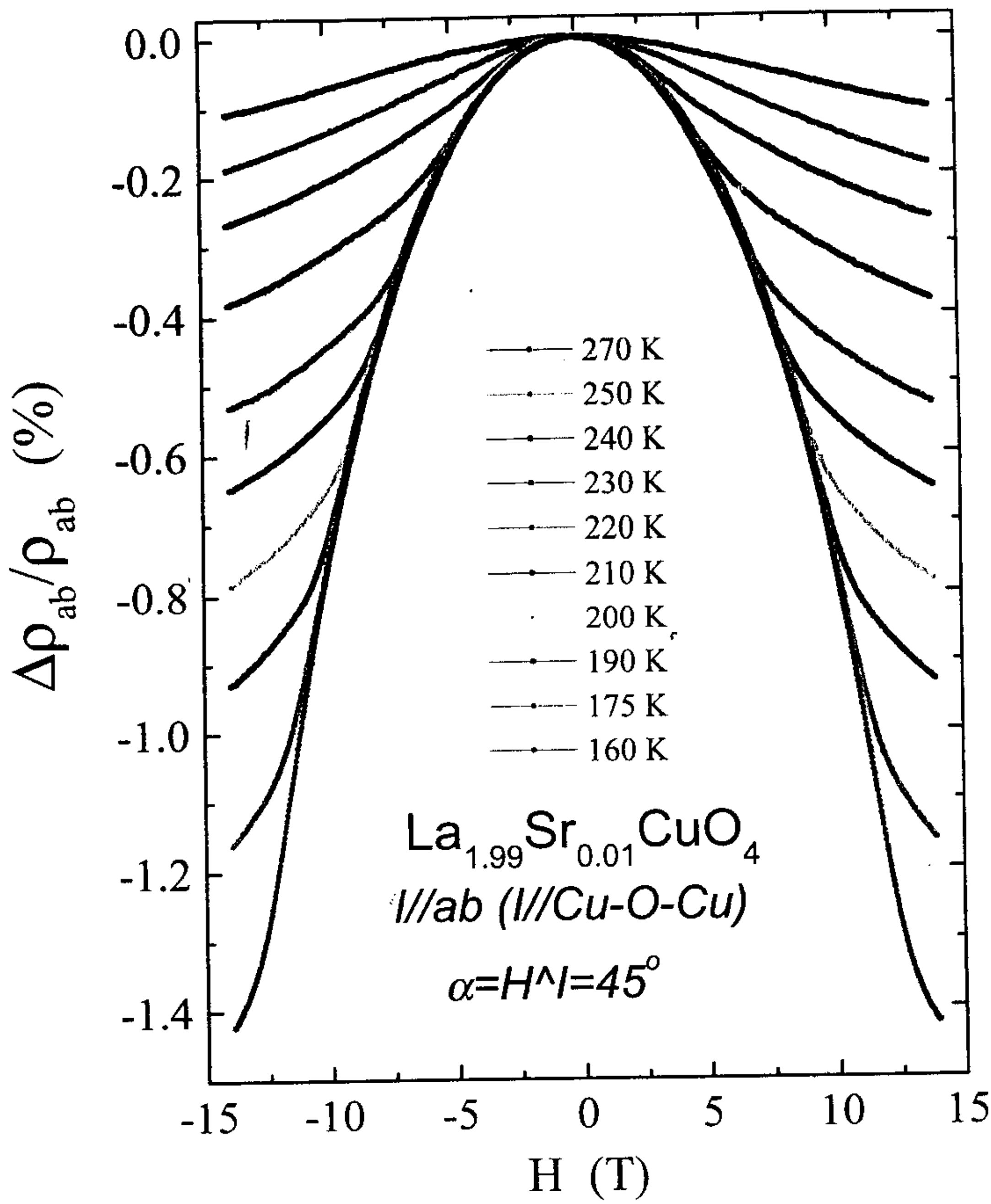

0.0
-0.2
-0.4
-0.6
-0.8
-1.0
-1.2
-1.4
$\Delta\rho_{ab}/\rho_{ab}$ (%)
270 K
250 K
240 K
230 K
220 K
210 K
200 K
190 K
175 K
160 K
$La_{1.99}Sr_{0.01}CuO_4$
I//ab (I//Cu-O-Cu)
$\alpha=H\hat{}I=45^o$
-15
-10
-5
0
5
10
15
H (T)

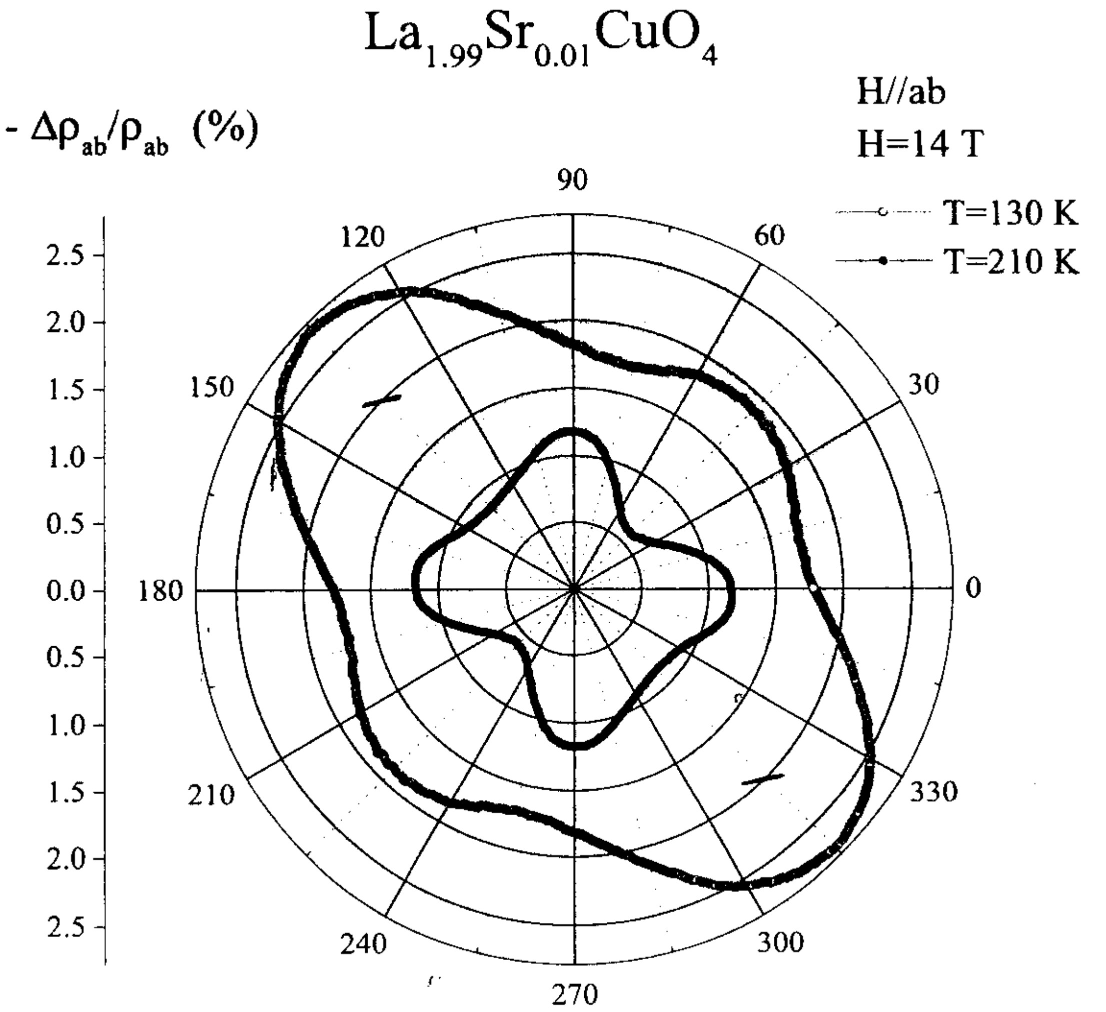
$La_{1.99}Sr_{0.01}CuO_4$
H//ab
H=14 T
$-\Delta\rho_{ab}/\rho_{ab}$ (%)
T=130 K
T=210 K
2.5
2.0
1.5
1.0
0.5
0.0
0.5
1.0
1.5
2.0
2.5
90
120
60
150
30
180
0
210
330
240
300
270

I // Cu-O-Cu

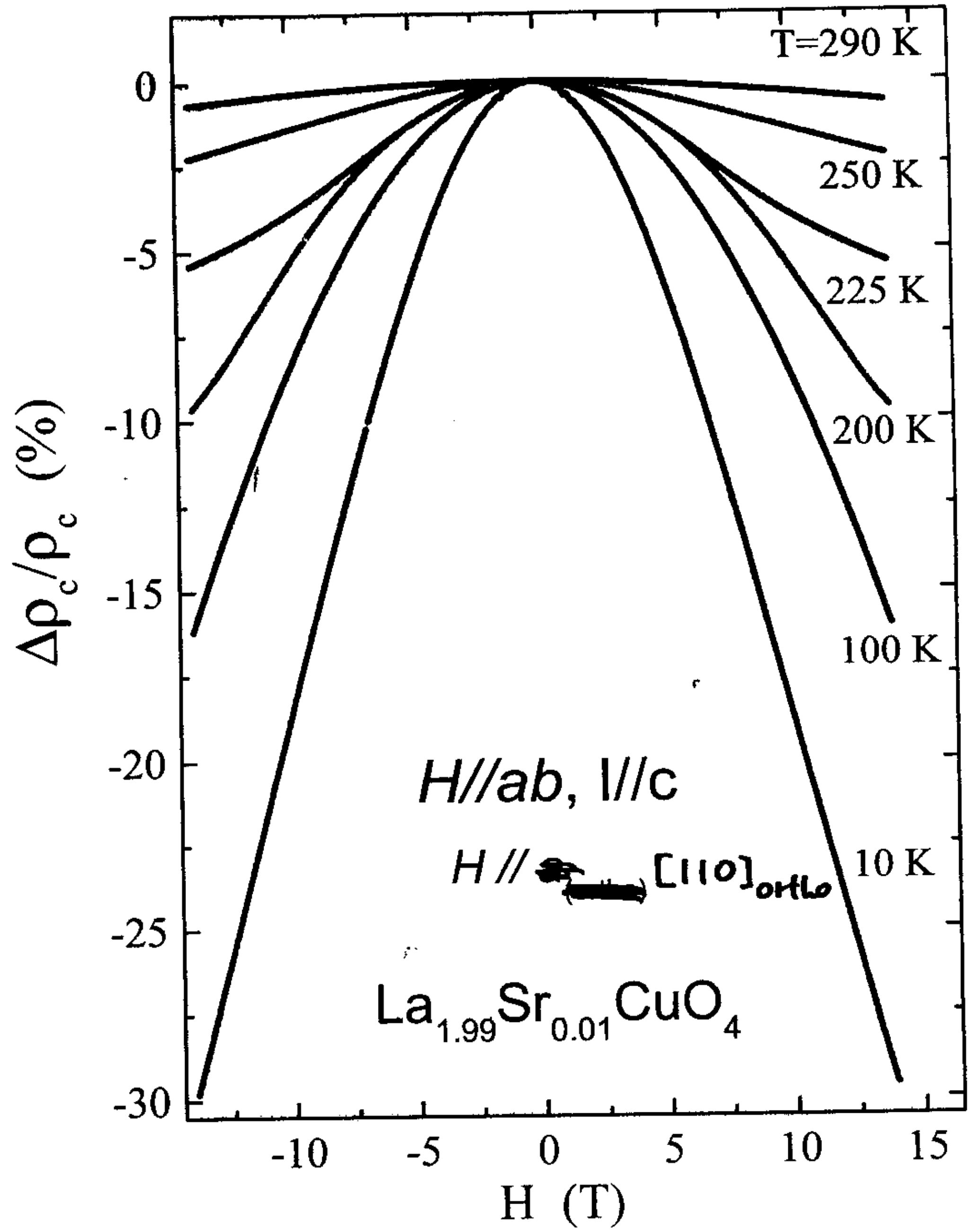
T=290 K
250 K
225 K
200 K
100 K
10 K
H//ab, I//c
H // [110]ortho
La1.99Sr0.01CuO4
Δρc/ρc (%)
H (T)
0
-5
-10
-15
-20
-25
-30
-10
-5
0
5
10
15

$La_{1.99}Sr_{0.01}CuO_4$

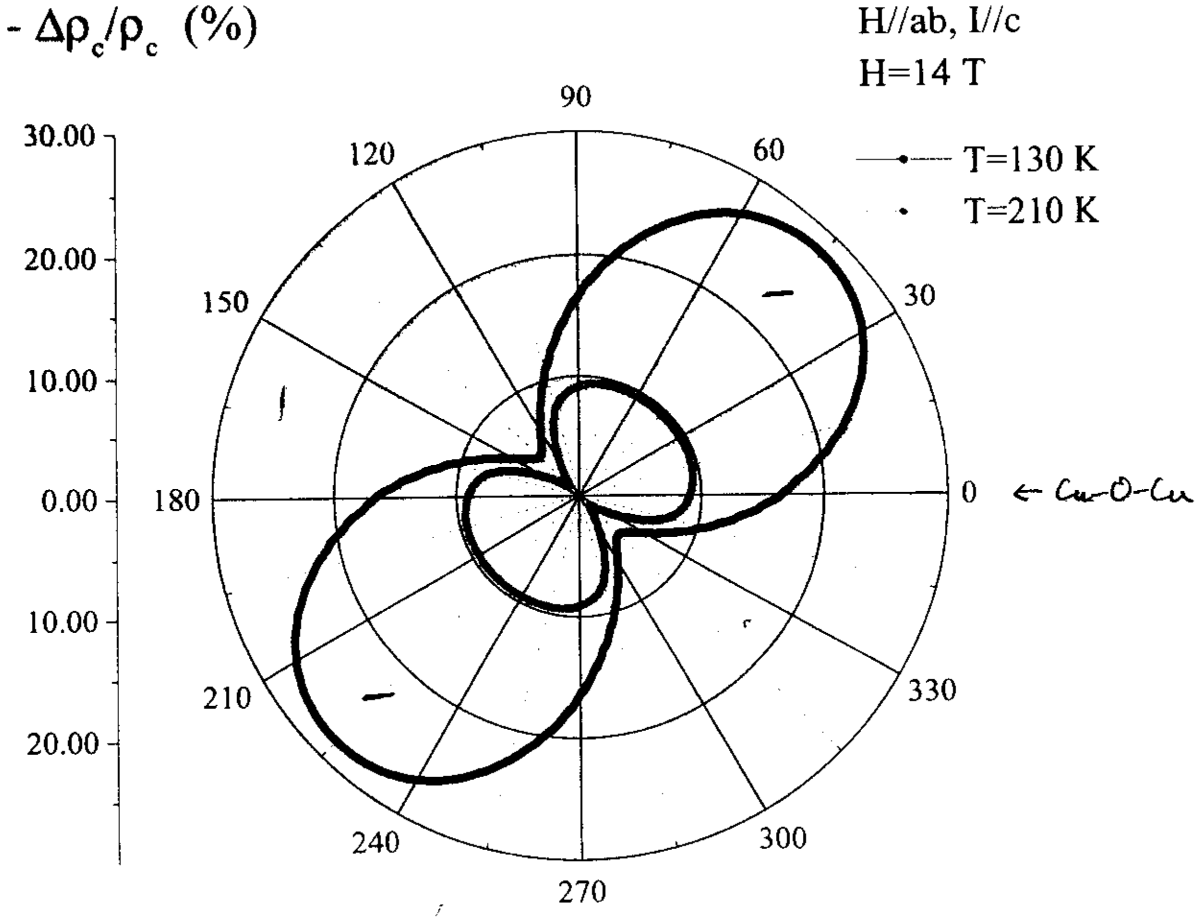

Summary

- **Sufficiently** underdoped cuprates show unusual **localization** behavior when SC is suppressed.

  ...*"Anomalous Insulator"*

- MI crossover is *not* universally associated with optimum doping.

- MI crossover and the "anomalous insulator" might be related to the static stripes.

- Doped carriers have almost universal *mobility* at moderate temperatures.
  Also, metallic ρ_{ab} is observed even in the Néel state.

  ...*"Anomalous Metal"*

- The anomalous metal is likely to be related to the dynamically fluctuating stripes.